Alma Mater Studiorum · Università di Bologna

Scuola di Scienze
Dipartimento di Fisica e Astronomia
Corso di Laurea in Fisica

Dynamical Models in Neuroscience: The Delay FitzHugh-Nagumo Equation

Relatore:
Prof. Armando Bazzani

Correlatore:
Dott. Giulio Colombini

Presentata da:
Chiara Zelco

Anno Accademico 2021/2022

"L'instruction! Voyez ce que c'est, monsieur, que l'instruction. On apprend quelque chose à l'école, on se donne même du mal, beaucoup de mal, pour apprendre quelque chose à l'école, et puis vingt ans après, ou même avant, ce n'est plus ça, les choses ont changé, on ne sait plus rien, alors vraiment ce n'était pas la peine. Aussi je préfère penser qu'apprendre."

Raymond Queneau, *Les Fleurs Bleues*

Abstract

Il primo modello matematico in grado di descrivere il prototipo di un sistema eccitabile assimilabile ad un neurone fu sviluppato da R. FitzHugh e J. Nagumo nel 1961. Per quanto schematico, esso rappresenta un importante punto di partenza per la ricerca nell'ambito neuroscientifico delle dinamiche neuronali. L'elevato grado di complessità che si riscontra nello studio dei neuroni e delle dinamiche inter-neuronali comporta, tuttavia, che molti aspetti di tale argomento non siano ancora state compresi appieno. In questo lavoro verrà approfondito un modello matematico di equazioni differenziali che riprende il lavoro originale di FitzHugh e Nagumo. Tale modello è ottenuto tramite una approssimazione di campo medio applicata ad una rete neuronale, permette dunque una descrizione semplificata degli stati macroscopici di un ensemble di neuroni. L'introduzione del ritardo è funzionale ad una descrizione più realistica di fenomeni neuronali e produce una dinamica maggiormente complessa rispetto a quella studiata nella versione originale del modello. Sarà mostrata l'esistenza di una soluzione a ciclo limite nel modello con termine di ritardo temporale, ove tale soluzione non può essere interpretata nell'ambito delle biforcazioni di Hopf. Si trarranno alcune conclusioni sul comportamento dinamico del sistema utilizzando simulazioni numeriche. Allo scopo di approfondire i metodi e le caratteristiche della modellizzazione del neurone, verrà principalmente utilizzata l'impostazione della teoria dei sistemi dinamici, integrando ove necessario con nozioni provenienti dall'ambito fisiologico. In conclusione sarà riportata una sezione di approfondimento sulla integrazione numerica delle equazioni differenziali con ritardo.

Contents

Chapter 1

Introduction

Neuroscience, and particularly the detailed study of neurons and of their reciprocal interactions, is a field of great interest both from a theoretical point of view and in an application perspective. The dynamical systems theory has had some luck in the last century in contributing to the advancement of the neuroscience study field, other than the classical physiological and molecular approaches.

Although the history of Neuroscience traces back to ancient times, the first modern intuitions can be temporally located between the eighteenth and nineteenth century, with the observations on the role of electricity in nerves and on the electrical excitability of neurons. During the twentieth century, neuroscience began to be considered as a distinct unified discipline in academic contexts, rather than studies of the nervous system previously carried out in separate scientific fields.

One of the most pressing questions of early twentieth century neuroscience concerned the physiology of nerve impulses. By the end of the second decade many relevant hypothesis had been advanced regarding the action potential generation mechanism (Julius Bernstein, 1902 and 1912), which was though to result from a change in the permeability of the axonal membrane to ions [1]. The Nernst equation for resting potential across the membrane was likewise first introduced in the same years, and, in 1907, Louis Lapicque suggested that the action potential was generated as a threshold was crossed [2]. This was the first step towards the introduction of a dynamical systems approach in neuroscience. During the same period, Keith Lucas carried out experiments on muscles contraction that led to the formulation of the *all-or-none principle* [3], which we will recall in the following.

The neuron action potential was first observed via a specifically modified oscilloscope by Josepht Erlanger and Herbert Gasser, who were able to identify the two phases that characterize such phenomenon. Bernstein's hypothesis about the action potential was eventually confirmed in 1939 by Kenneth Cole and Howard Curtis, who showed that membrane conductance increases during an action potential [4]. Cole was joined at the

Rockefeller Institute by Alan Lloyd Hodgkin, with whom he managed to measure the direct current resistance of the membrane of the squid giant axon in the resting state. After Cole developed the voltage clamp technique[1] in 1947, the time was ripe for the development of the Hodgkin and Huxley renowned mathematical model. Such model described the transmission, initiation and propagation of electric signals in neurons of the giant axon of a squid. Their work was the starting point of the FitzHugh–Nagumo model which is the study object of this work.

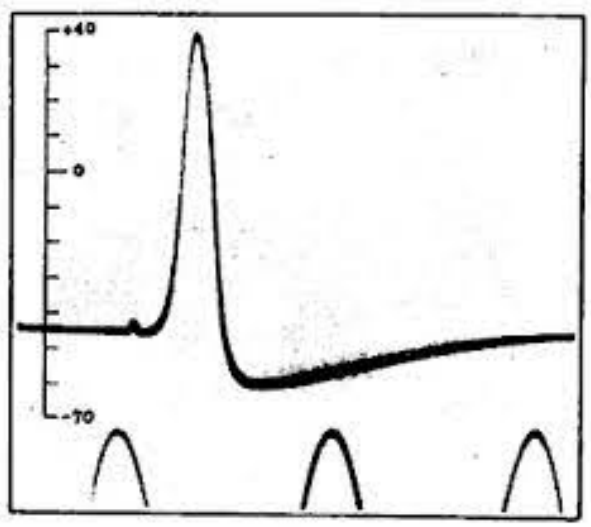

Figure 1.1: Intracellular recording of an Action Potential in the squid giant axon (Hodgkin and Huxley, 1939)

In the following years many advancements were witnessed in the neuroscience and neurocomputation fields, in particular with Bernard Katz's model of synapses and the studies biochemical changes in neurons associated with learning and memory storage of Eric Kandel et al., eventually combined in the 1981 Morris-Lecar model. The quantitative character of these works set the premises for the development of a great number of new biological neuron models and models of neural computation.

In parallel to the deepening of neuroscientific knowledge, the neural network sector started to flourish. One additional work that attempted to produce a mathematical model of a neuron was published in 1943 by neuro-physiologist and cybernetician Warren McCulloch and logician and cognitive psychologist Walter Pitts. Their idea was to describe brain functions in abstract terms, partly taking inspiration from Alan Turing's article "On Computable Numbers", showing that simple elements connected in a neural network can have immense computational power[5]. Still in the neural networks field, it

[1]The voltage clamp technique consists of an experimental method used to measure ionic currents across excitable cells membrane, while holding the membrane voltage at a set level.

would be a loss not to mention the concept of *perceptron*, developed by Frank Rosenblatt in 1958 and massively employed in subsequent research on neural networks.

In this work we will focus on what made the FitzHugh-Nagumo model especially relevant in the neuroscientific world, that is, the introduction of dynamical concepts which had not been extensively employed before. Initially it was (and in many cases still is) uncommon, in the study of neuroscience, to employ physical tools derived from nonlinear dynamical systems theory. The pioneering work in this sense was that of FitzHugh, who managed to introduce fundamental concepts such as equilibrium, stability, limit cycle attractor, and bifurcations in the analysis of neurons behavior. This practice allowed the discipline to gain a more top-down approach, allowing the models to be more predictive and giving them broader descriptive potential.

Shifting of the point of view towards physical sciences has had great success in terms of research, since it has allowed to transfer complexity from specific physiological problems, to the more general framework of dynamical systems. Many studies have moved their first steps starting from the FitzHugh-Nagumo model, making it more realistic by adding different features to it. Some have focused on the problem of neuron coupled and synchronization, others have added spatial partial derivative terms to account for the physical propagation of action potentials. The dynamics of these variations and of the original model itself, is extremely rich, and still presents some unresolved issues. In the case of the present work, the study will concern the introduction of a self-coupling term with a time delay, in a slightly simplified version of the original model. Such version serves as an average model that describes the macroscopic states of an ensemble of neurons, thus resulting to be a suitable tool for problems that involve multiple neurons.

The FitzHugh-Nagumo model is described by a bi-dimensional system of differential equations governing the dynamics of two variables, i.e, the membrane excitation variable and the recovery variable. The presence of the term with delay introduces some additional mathematical complexity, since the system features functions of variables both computed at present time and at a prior time as well, indeed individuated by the time delay term. Considering the nature of the model, the system needs to be described by suitable mathematical tools, which in our case are *delay differential equations*. The topic of such kind of differential equations is developed in Chapter 2. In Chapter 3 we first recall some physiological notions useful in the understanding of the model, referencing the work by Hodgkin and Huxley. We then follow FitzHugh's steps in the development of his dynamical model, tackling the subject of nonlinear oscillators with an overview on the model for the van der Pol oscillator. After an introduction to the dynamical model itself, some dynamical tools are introduced. We then present the notion of excitability of the neuron seen from a dynamical point of view, furthering the subjects of stability, equilibrium and bifurcations. This discourse is integrated with the presentation of some neurocomputational properties, regarding the existence of the firing threshold. The

knowledge gained on the van der Pol oscillator is revealed to be profitable in Chapter 3, which concerns the study of a simplified version of the FitzHugh-Nagumo model. In Chapter 4 the self-coupled term with time delay is introduced in the equations system. Several simulations are performed on the system to understand its behavior and how its dynamical framework changes compared to the model with no time delay term.

The first test we perform considers the variation of the system parameters, and in particular we act on the coupling constant and time delay terms. We make some considerations on the dynamical behavior of the system under a joint variation of both parameters. The focus is posed on when and where the quasi-threshold of the system is reached in terms of coupling constant and time delay values. Exploiting the simulations, we extract the shape of the delayed variable plotted against time, and study how it changes in case the systems is in the stable limit cycle or in the stable equilibrium configuration. We then concentrate on the spiking state of the modelized neuron, and study how the area circumscribed by the limit cycle changes at every next iteration. We find that the trend of the areas possesses an asymptote, which is reached exponentially fast.

Chapter 2

Motivation for Delay Differential Equations

Delay differential equations have become a topic of growing importance in the complex systems and dynamical systems field of study. These types of differential equations differ from ordinary differential equations in that the derivative at any time depends on the solution at prior times. The simplest constant delay equations have the form

$$y'(t) = f(t, y(t), y(t-\tau_1), y(t-\tau_2), \ldots, y(t-\tau_k)). \tag{2.1}$$

The success and the growing interest in this topic can be explained considering the intrinsic nature of many processes found in nature, that is, *they take time to complete!* Biological process times, such as gestation periods and maturation times, for example, can be substantial when compared to the data collection times in most population times. This is also true for control theory applied to mechanics and traffic studies. The need to develop suitable mathematical instruments to study these processes has led to growing interest in the field of delay differential equations (DDEs in the following).

Recent theoretical and computational advancement revealed that DDEs are capable of generating rich and plausible dynamics with realistic parameter values. Naturally occurring complex dynamics are often generated by well formulated DDE models [6].

Perhaps one of the most analyzed and most popular dynamical models is the Lotka-Volterra predator-prey model, initiator of many ecology and populations studies. Less known, but particularly relevant to this subject, is the Nicholson's blowflies model, developed as a variation on Lotka-Volterra to model laboratory flies population in a more true-to-life way. The element that contributes to making the model more realistic is indeed the introduction of delay terms in the equation [7]. A reasoning along these lines was carried out to produce a variation of the likewise renowned logistic equation, which

finds applications in a wide range of study fields. It is generally assumed that organisms' birth and/or death rates respond instantaneously to changes in population sizes, however, there are some organisms that have some lag time before they reproduce again. Hutchinson was one of the first mathematicians to introduce a delay into the logistic equation to account for hatching and maturation periods [8], with the aim of obtaining a more realistic model and a more complex dynamic in return. In the following, the original logistic equation 2.2, continuous version of the logistic map, and Hutchinson's delayed logistic equation 2.3 are shown:

$$\frac{dy(t)}{dt} = y(t)(1 - y(t)) \tag{2.2}$$

$$\frac{dy(t)}{dt} = \alpha y(t) \left(1 - \frac{y(t-\tau)}{K}\right), \tag{2.3}$$

where $\tau > 0$; K denotes the carrying capacity of resources, and α denotes the intrinsic growth rate.

The need to include lag times in ecological models is not the only field where DDEs are being employed and further developed. DDEs are fruitfully employed also in models which require the introduction of some kind of *feedback*. When the concept of control is involved, as it often happens when modeling automatic engines or physiological systems, feedback becomes central, because it is used to maintain a stable state.

Previously known equations are investigated allowing better physical understanding of old problems. In addition, new areas of research are being explored. It is the case of lasers subject to optical feedback, delayed control of automatic engines and traffic stability studies.

The concept of feedback is massively employed in physiology and in the study of neural systems. There are several sources of delay in a neural system. The most immediate one is the delay due to propagation of rapid rises and falls in membrane potentials (which will be called *action potentials* in the following) along the axon, while another is the transmission of the electrical signal across the synapse. In simple models, when an action potential is generated in the cell body of a neuron, it is immediately felt by all other neurons to which it is connected. However, in reality, the action potential must travel along the axon of the first neuron to the synapse or gap junction. Conduction velocities can range from $1m/s$ to $100m/s$ depending on the constituents that make up the sheath of the nerve fiber. When neural systems are considered, the simplest approach is to include a time delay in the differential equations term describing the coupling of different neurons[9].

It is custom in the study of neural systems to write the coupling function of neurons, for example in the case of the j^{th} neuron being connected to the i^{th} via a chemical synapse

we would have

$$f_{ij}(\mathbf{y}_i(t), \mathbf{y}_j(t)) = c_{ij} g_{ij}(\mathbf{y}_j(t)) h_{ij}(\mathbf{y}_i(t)). \tag{2.4}$$

If the previously mentioned sources of delay are considered, the function can be modified by including the constant delay $\tau_{ij} > 0$, this simple approach returns a function in the following form:

$$f_{ij}(\mathbf{y}_i(t), \mathbf{y}_j(t - \tau_{ij})) \tag{2.5}$$

More variations can be applied to modify the model and make it more suitable for different situations. It is possible, for example, to consider time dependent delays $\tau_{ij}(t)$, or to introduce noise in the delay terms.

Other than in the neural systems framework, the introduction of time delays is particularly successful in the scope of neural networks, which sometimes also have parallels with biological neural networks[9].

When one wants to formulate a model to describe areas of the brain, one of the most common approaches is to consider neuronal networks, i.e. sets of neurons which interact with one another according to a network structure that specifies their couplings. The mathematical-physical framework that allows this kind of study is the theory of networks. Depending on the scale of the considered system, we might have to account for the role that the distance between neurons plays. For example, a study in the mesoscopic scale should feature a time delay to account for impulse transmission times. When one is studying the emergence of collective phenomena, a reasonable first approximation can be obtained by neglecting the connectivity fluctuations present in the network. Doing so, one obtains an equation for the average behavior of the network which corresponds to a single neuron with feedback [10]. The FHN model with delay is indeed the result of this approach.

In the specific case of the delayed-FHN model, the delay cannot in fact directly be ascribed to the presence of other neurons or of a network, as it is the result of applying the Mean-field theory to a network of neurons. The study of the solutions observed for this model, however, has some applicability to the fore-mentioned cases. The delay is employed by the system to become self-sustained, for example, as we will see, to remain in the excitable phase when no external impulse is given.

The aim of this work is to present the dynamical model describing simple neuron dynamics developed by R. FitzHugh and J. Nagumo. The focus will be on the study of the neuron model as a feedback phenomenon, introducing a delay term in the system of differential equations presented in FitzHugh's original paper [11].

2.0.1 Properties of DDEs

Before going into the details of the FHN model, it is useful to substantiate the general Delay Differential Equations framework. There are two important properties of DDEs

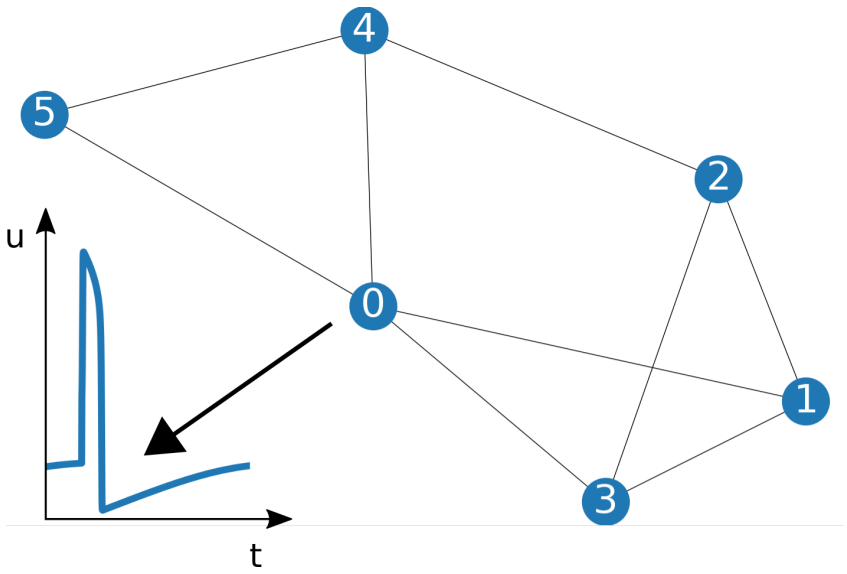

Figure 2.1: Schematic depiction of a neurons network. A first approximation result in an equation for the average behavior of the network which corresponds to a single neuron with feedback. The spike of the single neuron is shown on the left. Courtesy of Giulio Colombini.

that need to be stressed. For one, their solutions can be oscillatory, in contrast to those of single ordinary differential equations. This is because the single DDE is not 1-dimensional, but is actually infinite dimensional. This comes as no surprise, since the value of y must be specified over an entire interval to initialize the DDE [12].

The oscillatory behavior can be observed in the solution of the previously mentioned Nicholson model, evolution of Lotka-Volterra, for example. This marks one difference with the latter model, that possesses a much less complicated dynamics and does not present oscillations in its solutions.

The second fundamental aspect is that to initialize DDEs, not only initial conditions are required, but also the equations' "history". History is the common way to refer to the solution $y_0(t)$ at times prior to the initial point. Many mathematical methods have been developed regarding how the effect of $y_0(t)$ can be investigated. In general, the presence of the initial history is solved numerically.

Because numerical methods of both ODEs and DDEs are intended for problems with solutions that have several continuous derivatives, discontinuities in lower order derivatives require special attention. Having a discontinuity in the first derivative at a certain time can mean that such jump propagates to a jump in the second derivative at the next time step, and so on. More generally, the jump in $\dot{y}$ at time $t = m$, propagates to a jump in $y_{n+1}(t)$ at time $t = m + n$. In summary, a long-time oscillatory solution is possible and initial history may have an effect on the short-time solution [8].

The model whose study is the object of this work is characterized by a feature that makes its integration a quite challenging task. As will be addressed in the following, the presence of a small parameter multiplying one of the equations of the DDEs system, entails that the system must be treated as "stiff". A description of stiffness is given in Appendix A.

Chapter 3

The FitzHugh-Nagumo Neuron Model

The main interest of this work is to gain some knowledge about the models developed to describe mathematically the neuron and its physiological features, with a focus on the field of dynamical systems.

There is a significant advantage in using a physical-mathematical theory to describe neurons and their coupled behavior, because it allows to subsume a considerable variety of phenomenological manifestations in possibly very few dynamical categories. Recognizing those categories and the reason why they form eventually leads to a better understanding both of the big-picture and of the single phenomena and processes.

From the neuroscience perspective, it was a big step forward coming to the conclusion that "*information-processing depends not only on the electrophysiological properties of neurons but also on their dynamical properties*". Neurons with similar electrophysiological features "*may respond in different to the same synaptic input in very different manners because of each cell's bifurcation dynamics*"[13]. The concept of bifurcation dynamics will be later further developed.

Before diving into the dynamical description of the model, we need to acquire some physiological notions about neurons, the way they activate and communicate with the rest of the nervous system.

3.1 The Hodgkin and Huxley model

We now concentrate on the Hodgkin and Huxley model of the squid giant axon (1952), one of the most important models in computational neuroscience. Widely considered representative of the general dynamics of neurons, it describes how action potentials are initiated and propagated. It is a set of nonlinear differential equations that approximates

the electrical characteristics of excitable cells such as neurons and muscle cells.

Electrical activity in neurons is sustained and propagated via ionic currents through neuron membranes. The cell membrane is a double layer of phospholipidic molecules forming channels through which ions can flow according to the electrochemical gradients, generated by the different concentration of ions in the intra-cellular and extra-cellular medium. The ion species that are relevant to this dissertation are: sodium Na^+, chloride Cl^- and calcium Ca^{2+}, that populate in higher concentrations the extra-cellular medium, potassium K^+, more abundant on the inside of the cell, as well as negatively charged molecules (denoted by A^-).

Concentration gradients and electrical potential gradients are, in summary, the two forces that drive each ion species through the membrane channel. This might be called passive transport, as opposed to the active transport performed by ionic pumps, that tend to maintain concentration gradients, and to passive redistribution, by which the anions A^-, too large to permeate the membrane, attract more K^+ into the cell and repel more Cl^- out of the cell, thereby creating concentration gradients.

The mixed effect of these processes eventually leads to an equilibrium: the concentration gradient and the electric potential gradient balance each other, and the net cross-membrane current is zero. The value of the equilibrium potential (the Nernst potential) depends on the ionic species, and is given by the Nernst equation.

A useful tool to study the activity of the neuron is to build an equivalent circuit out of the electrical behavior of the membrane and of ionic flows. In the following, V denotes the membrane potential, and E_{Na}, E_{Ca}, E_{Cl} and E_K the Nernst equilibrium potentials. $C\dot{V} = I - g_{Na}(V - E_{Na}) - g_{Ca}(V - E_{Ca}) - g_{Cl}(V - E_{Cl}) - g_K(V - E_K)$

When the membrane potential equals the equilibrium potential, the net current, denoted by I, is zero. The g_{Na}, g_{Ca}, g_{Cl} and g_K parameters are also introduced to represent the conductances of the membrane with respect to the chemical species. In general, ionic currents are not Ohmic, i.e. the conductances are not constant. In fact, conductances may depend on time, membrane potential and pharmacological agents. Most importantly, it is the time-dependent variation in conductances that allows neurons to generate an action potential. In fact, if the ionic channels were Ohmic, the system would simply relax to a weighted average of the Nernst potentials V_rest.

According to Kirchhoff's law, the total current, I, flowing across a small area of a cell membrane is given by the sum of the membrane capacitive current $C\dot{V}$ and all the ionic currents:

$$I = C\dot{V} + I_{Ca} + I_{Na} + I_K + I_{Cl} \tag{3.1}$$

The voltage derivative arises because some time is required to charge the membrane. If there are no additional current sources or sinks, then $I = 0$.

As experimentally determined by Hodgkin and Huxley, the squid axon carries three major currents:

1. voltage-gated K^+ current with four activation gates (resulting in the n^4 term found

in the equation below, where n is the activation variable for K^+);

2. voltage gated Na^+ current with three activation gates and one inactivation gate (the m^3h term);

3. Ohmic leak current, I_L, carried mostly by Cl^- ions.

The n^4 term is the activation variable for K^+, m stands for the probability of an *activation* gate being open, and h of an *inactivation* gate being open. The complete set of the Hodgkin-Huxley dynamical equations is

$$C\dot{V} = I - \bar{g}_K n^4 (V - E_K) - \bar{g}_{Na} m^3 h (V - E_{Na}) - g_L (V - E_L) \tag{3.2}$$

$$\dot{n} = \alpha_n(V)(1 - n) - \beta_n(V)n \tag{3.3}$$

$$\dot{m} = \alpha_m(V)(1 - m) - \beta_m(V)m \tag{3.4}$$

$$\dot{h} = \alpha_h(V)(1 - h) - \beta_h(V)h, \tag{3.5}$$

where

$$\alpha_n(V) = 0.01 \frac{10 - V}{\exp(\frac{10-V}{10}) - 1}, \tag{3.6}$$

$$\beta_n(V) = 0.125 \exp(\frac{-V}{80}), \tag{3.7}$$

$$\alpha_m(V) = 0.1 \frac{25 - V}{\exp(\frac{25-V}{10}) - 1}, \tag{3.8}$$

$$\beta_m(V) = 4 \exp(\frac{-V}{18}), \tag{3.9}$$

$$\alpha_h(V) = 0.07 \exp(\frac{-V}{20}), \tag{3.10}$$

$$\beta_h(V) = \frac{1}{\exp(\frac{30-V}{10}) + 1}, \tag{3.11}$$

These parameters where provided in the original Hodgkin and Huxley paper. They correspond to the membrane potential shifted by approximately $65mV$, so that the resting potential is at $V \approx 0$.

3.1.1 Action Potential

When the potential equals V_{rest}, in correspondence to $0mV$ in the Hodgkin-Huxley model, all inward and outward currents balance each other so that the net current is zero, this is the resting state. Such resting state is a stable point: a small pulse of current produces a slight depolarization of the membrane, a slight positive perturbation; the depolarization produces a small net current, and the system is driven back to rest state (repolarization).

If the current pulse has a bigger size, the effect is quite different, thanks to the non-linearity of the conductances-potential relation. In the latter case, an action potential is formed, i.e., the produced perturbation is amplified significantly. If we were to plot the behavior of the system against time, in this case we would observe a marked growth for the excitable variable, a spike, followed by a sharp fall that brings the variable below zero, in a phase called *refractory period*. A depiction of an action potential is shown in Figure 3.1. This happens because the recovery of some membrane variables is relatively slow. In particular, the K^+ current continues to be activated even after the action potential down-stroke, thereby causing V to go below V_{rest}. This phenomenon, known as *afterhyperpolarization*, corresponds to the *absolute refractory* period, where the HH system cannot generate another action potential, and to the *relative refractory* period, where the system becomes able to generate a new action potential, provided the stimulus is relatively strong.

Some studies have tackled the topic of the propagation of action potentials. In this case, the space variable x ought to become a system variable, and the partial derivative of the potential with respect to x is added to the voltage equation. The type of solution obtained by the model is quite remarkable, and it is called the Hodgkin-Huxley cable or propagating equation.

3.2 Oscillators and Phase Plane Description

Due to its highly nonlinear dynamics, the HH model exhibits a wide variety of possible behaviors, difficult to study in four dimensions and possibly chaotic. For this reason, a more manageable model was later independently developed by Richard FitzHugh (1961) and Jinichi Nagumo and al, who created the equivalent circuit of the system in the following year.

The FitzHugh-Nagumo (FHN) model mainly consists of a sensibly chosen two-dimensional projection of the four-dimensional original model. It still possesses the relevant dynamical features while it gains in simplicity with the reduction to two dimensions, that allows the system to be studied in the phase plane.

The main interest of the FHN model is that it aims to serve as a simple representative of a class of non-linear systems which exhibit an excitable and oscillatory behaviour, in-

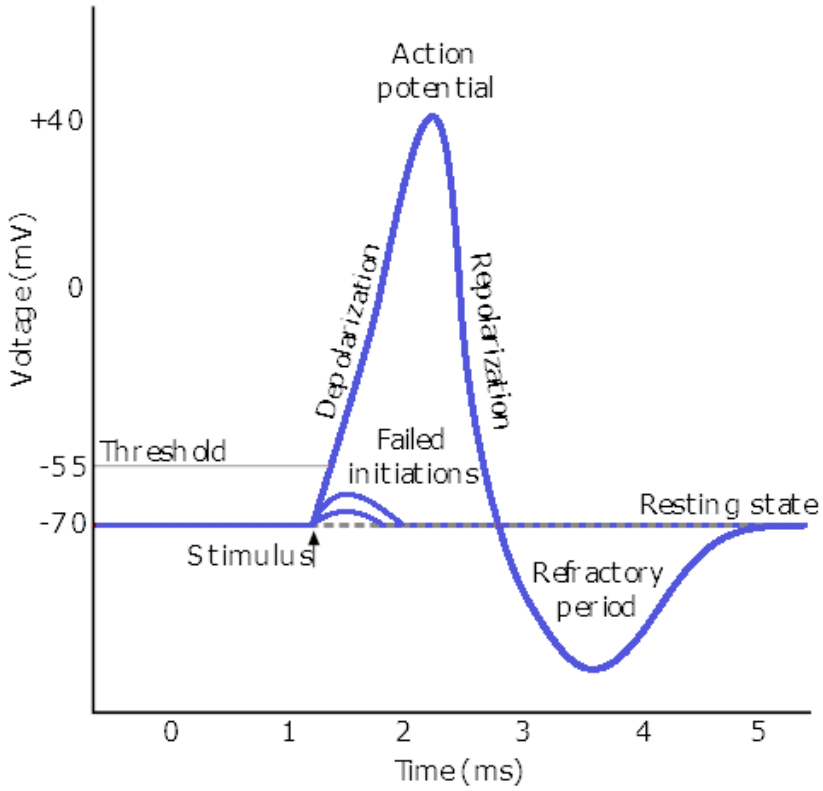

Figure 3.1: Schematic representation of an action potential. Original by Wikimedia Commons, CC BY-SA 3.0 [14]

cluding the Hodgkin-Huxley (HH) model of the squid giant axon. In his renowned paper, FitzHugh demonstrated that it was possible to describe the system as a generalization of the van der Pol (1926) equations for the relaxation oscillator [11].

The work on non-linear oscillators was at that time happening in parallel to the studies which aimed to generalize electrophysiological observations, and that eventually led to the HH model. The van der Pol oscillator does not give an accurate fit to curves obtained from physical oscillators, and the equation was rather intended to represent qualitative properties of a wide class of oscillators. Hence, being a classic example of a self-oscillatory system, it is considered a simple but rich starting point for many more complicated mathematical models[15].

In the following, we will give a brief exposition of the noteworthy dynamical features of the van der Pol oscillator, as they have some relevance in the interpretation of the non-delayed FHN model as well.

3.2.1 Van der Pol Equation

The governing equation of the van der Pol system is displayed below:

$$\frac{d^2x}{dt^2} - \mu(1 - x^2)\frac{dx}{dt} + x = 0 \ . \tag{1}$$

The equation presents nonlinear damping, clearly given by the multiplication of $\frac{dx}{dt}$ by the non-linear term $\mu(1-x^2)$, where $\mu > 0$ is a parameter, and x is a one-dimensional dynamical variable.

The system becomes approximately linear when negative damping $-\mu\frac{dx}{dt}$ – which corresponds to an amplification - is obtained. This is true when x is small, since the quadratic term becomes negligible. In this situation the fixed point ($x = 0, \frac{dx}{dt} = 0$) is unstable. On the other hand, when x grows, the damping becomes positive, which leads to an effective friction-like effect. In this case the quadratic term is dominating[16].

The van der Pol system 1 exhibits an oscillatory behavior, where the oscillations may be periodic or non periodic. It is possible to demonstrate that the system possesses one unique limit cycle enclosing the origin, and that limit cycle is asymptotically stable. In fact, the system satisfies Liénard's theorem[1], which ensures that there is a stable limit cycle in the phase plane. The system therefore is a Liénard system. The magnitude of parameter μ plays a role in determining the shape of the limit cycle. As shown in Figure 3.2, the shape is circular only in the case of $\mu = 0$, while it becomes progressively more elongated as μ grows.

Rewriting the system as done in Steven H. Strogatz's work [17] (calculations will not

[1]Liénard's theorem may be formulated as follows:

Liénard's Theorem. *If*

- $f(x)$ *is an even function for all* x,
- $g(x)$ *is an odd function for all* x,
- $g(x) > 0$ *for all* $x > 0$,
- $F(x) = \int_0^x f(t)dt$ *is such that* $F(x) = 0$ *has exactly one positive root* γ,
- *and* $F(x) < 0$ *for* $0 < x < \gamma$ *and* $F(x) > 0$ *and non-decreasing for* $x > \gamma$,

then the system

$$\dot{x} = y, \qquad \dot{y} = -f(x)y - g(x) \tag{3.12}$$

or, equivalently,

$$\frac{d^2x}{dt^2} + f(x)\frac{dx}{dt} + g(x) = 0 \tag{3.13}$$

has a unique limit cycle enclosing the origin and that limit cycle is asymptotically stable.

When all the conditions stated above are satisfied, as it happens for the van der Pol equation in the correct configuration of parameters, all system's trajectories spiral to the periodic solution as $t \to \infty$.

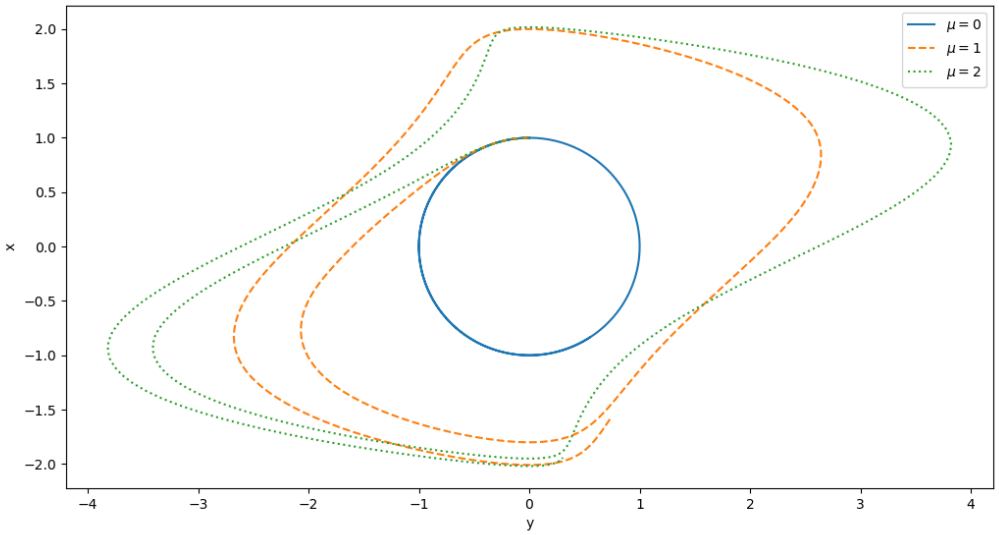

Figure 3.2: Phase plane of the van der Pol oscillator. The equations are integrated for three values of μ: 0, 1, 2. For different values of the parameter the solutions enter differently shaped periodic attractors called limiting cycles.

be reported here for the sake of the text flow) the $\dot{x}$ and $\dot{y}$ curves are obtained, here shown in the strongly nonlinear case, that is, when $\mu >> 1$.

$$\dot{x} = \mu \left(y - \frac{1}{3}x^3 + x \right) \tag{3.14}$$

$$\dot{y} = -\frac{x}{\mu} \tag{3.15}$$

This is the first time that we explicitly meet equations of the kind written in 3.15. The curves described by $\dot{x} = 0, \dot{y} = 0$ are nullclines of the system, which are curves in the phase plane where the vector field defined by the differential equation points in a particular direction. The former is the vertical motion nullcline, the latter is the horizontal motion nullcline. Points in the phase plane where nullclines cross are equilibrium points. Stability can be studied through linearization of the system in a surrounding of such points.

It is useful to study the phase plane and the nullclines to extract relevant information about the dynamics, a reference picture is shown in Figure 3.3.

Every trajectory that starts at a point different than the origin is forced by stability properties of the system to zap on the cubic nullcline. From there, the point follows along the nullcline until it comes to the "knee" (point B in the figure), after which it zaps over to the other branch of the cubic (point C). This is followed by another trait

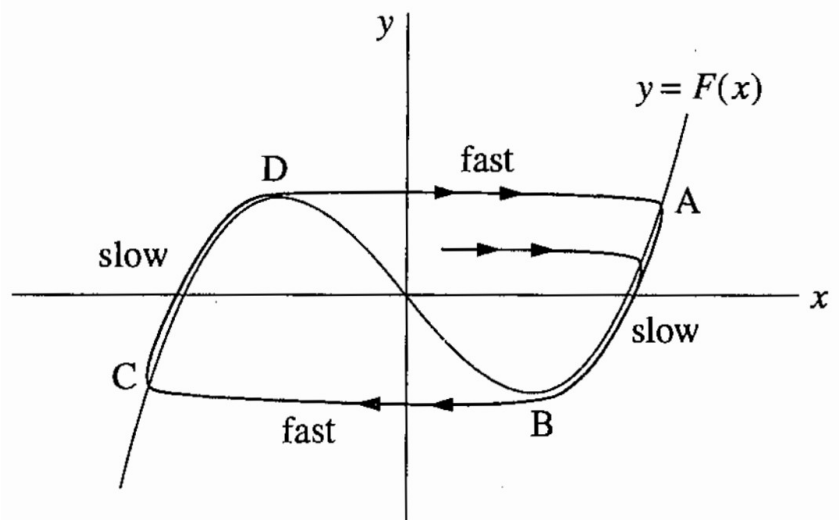

Figure 3.3: Nullclines of the van der Pol model. The limit cycle is shown. From S.H. Strogatz. *Nonlinear Dynamics and Chaos: With Applications to Physics, Biology, Chemistry, and Engineering.* CRC Press, 2015.

along the nullcline, until the trajectory reaches the other jumping-off point at D, and the motion continues periodically thereafter, traveling the limit cycle. The velocity is very high in the "horizontal" direction and much smaller in the "vertical" direction. Horizontal branches of the cubic nullclines are attractive for the trajectories.

This analysis shows the relaxation-oscillation dynamical behavior of the system and the appearance of a stable limit cycle. In fact, in the case of $\mu >> 1$, the limit cycle is governed by two widely separated time scales, as if stress was accumulated in the slow phase, and suddenly released when reaching points A, B, C and D, the jumping-off points. In this case different time scales operate sequentially (in other dynamical systems they might operate concurrently).

It can be shown that the motion along the horizontal branch takes $\Delta t \sim O(\mu)$, and the jumps take $\Delta t \sim O(\mu^{-1})$[17].

As an historical footnote, it is interesting that the authors of the studies on the oscillator (van der Pol and his colleague van der Mark) noted the appearing of "irregular noise" during regime transitions of the system. This is generally recognized to be one of the first observations of chaotic oscillations in the study of electronic devices. Their paper is probably one of the first experimental reports of chaos, although they were not able to correctly interpret the phenomenon, which would have been furthered only years later.

3.3 Dynamical Framework of the FHN Model

The FHN model was developed much in the same spirit as the van der Pol equation, aiming to represent a wider class of non-linear systems that show a stable state and threshold (or rather, quasi-threshold) phenomena, as well as stable oscillations.

Among the possible formulations of the problem we choose, for the sake of simplicity, the following one:

$$\varepsilon \dot{u}(t) = u(t) - \frac{u^3(t)}{3} - v(t) + I_{ext}(t) \tag{3.16}$$

$$\dot{v}(t) = u(t) + a \tag{3.17}$$

This formulation of the problem shares many characteristics with the van der Pol equation, i.e., the manifestation of two different time scales, depending on the magnitude of ε, and the shape of the nullclines, which entails the presence of the limit cycle. In particular, the I_{ext} function, characterizing the external stimulus, plays a fundamental role in the differential equations system.

Initially, we will briefly explore the case of the stimulus being a function of time, $I_{ext}(t)$, possibly representing currents given by the interactions with other neurons, or by external stimuli. With this setup, we will already observe the appearing of the periodic spiking behavior. Later on, we will deepen the response of the system in presence of feedback phenomena, i.e. when the stimulus term at time t is given by the neuron membrane potential itself, at a previous time. In this case, the excitation term is given by

$$I_{ext}(t) = J(u(t-\tau) - u(t)) \ , \tag{3.18}$$

where J is the coupling term of the system, and time delay is represented by τ.

The pair of differential equations turns in this case into a system of delay differential equations. The topic of DDEs' has already been tackled in the dedicated introductory paragraph2.

As previously noted, the basics of the dynamical system, even though the FHN model easily manifests much richer dynamical features, are described fairly well by the van der Pol equation. In fact, the remarkable aspects are the presence of the cubic nullcline, and the fact that the system possesses two widely different time scales.

Before analyzing equations 3.16 and 3.17 in depth, some useful dynamical tools will be introduced, trusting the fact that the overall qualitative description of the dynamics can be obtained through the study of the phase plane of the system. The presence of relevant dynamical and geometrical features such as equilibria, separatrices and limit cycles, determines the topological behavior of all other trajectories in the phase plane.

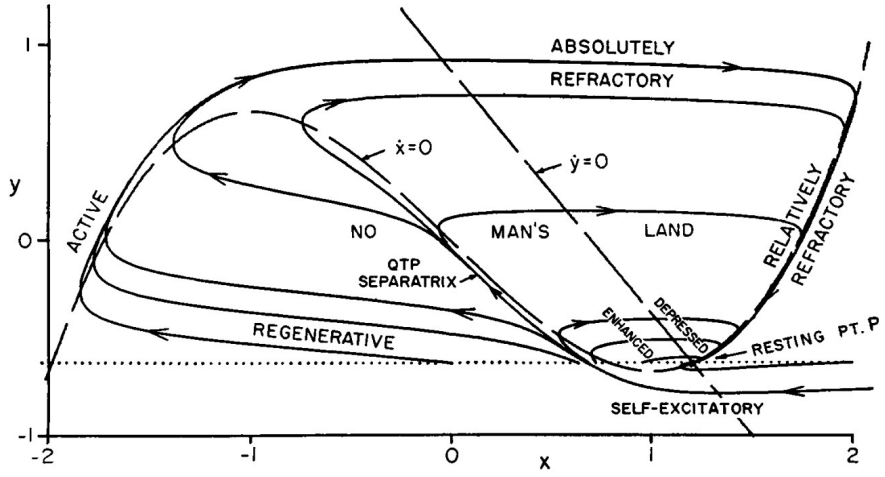

Figure 3.4: Phase plane and physiological state diagram of FHN model. The broken lines, represent the x and y nullclines. The dotted line is the locus of initial conditions following instantaneous external stimulus at rest. Labeled zones form physiological state diagram. R. FitzHugh 1961, *Impulses and physiological states in theoretical models of nerve membrane*, From the National Institutes of Health, Bethesda.

Let us then go further in depth in the analysis of these phase portrait elements.

A fundamental property of neurons is *excitability*. For starters, we will consider a resting neuron. Since it is resting, its phase portrait has a stable equilibrium. Small perturbations result in small excursions from the equilibrium, larger perturbations are amplified by the neuron's intrinsic dynamics and result in the spiking response. To understand the dynamical mechanism that leads or does not lead to an amplification of the incoming signal, we need to consider the geometry of the phase portrait near the resting equilibrium, i.e., in the region where the decision to fire or not to fire is made. If a sufficiently strong current is injected, the neuron is brought to a pace-making mode, so that it exhibits periodic spiking activity. From the dynamical systems point of view, the state of such a neuron has a stable limit cycle, also known as a stable periodic orbit. Equilibria and limit cycles can coexist, so a neuron can be switched from one mode to another by a transient input.

So far, we only considered two distinct dynamical states of the neuron, i.e., resting and spiking mode. If we treat the magnitude of the injected current as a parameter that can be controlled, we expect to encounter an intermediate level of injected current that corresponds to the transition from resting to sustained spiking. The transition corresponds to a bifurcation of neuron dynamics. Returning now to the concept of excitability, in general, *neurons are excitable because they are near bifurcations* of this kind [13]. The type of bifurcation therefore determines the excitable properties of the neuron.

3.3.1 Bifurcations

A system is said to undergo a bifurcation when its phase portrait changes qualitatively. The type of bifurcation depends on the neuron's electrophysiology. Notwithstanding the huge number of possible different electrophysiological mechanisms of excitability and spiking, there are only four types of bifurcations that a system can undergo without any additional constraints such as symmetry.

In the following, we will briefly summarize the characteristics of the four types of *codimension-1* bifurcations of equilibria, i.e., those which only need the variation of a single parameter to be observed.

- *Saddle-node bifurcation.* As the magnitude of the injected current or any other bifurcation parameter changes, a stable equilibrium, corresponding to the resting state, is approached by an unstable equilibrium; they coalesce and annihilate each other. Since the resting state no longer exists, the trajectory that describes the evolution of the system moves to the limit cycle attractor. The limit cycle, or some other attractor[2], must coexist with the resting state in order to let the transition from resting to spiking occur.

- *Saddle-node on invariant circle bifurcation* is similar to the saddle-node bifurcation except that there is an invariant circle at the moment of bifurcation, which then becomes a limit cycle attractor. Both in this kind of bifurcation and in the former, resting and spiking states coexist.

- *Subcritical Andronov-Hopf bifurcation.* A small unstable limit cycle shrinks to a stable equilibrium and makes it lose stability. Because of instabilities, the trajec-

[2]In general, an attractor is defined as a subset A of the phase space characterized by the following three conditions:

- A is *forward invariant* under the function $f(t,(x,v))$ describing the evolution of the system in phase space: if a is an element of A then so is $f(t,a)$, for all $t > 0$
- There exists a neighborhood of A, called the basin of attraction for A and denoted $B(A)$, given by all points that belong to A in the infinite-time limit. More formally, $B(A)$ is the set of all points b in the phase space with the following property: For any open neighborhood N of A, there is a positive constant T such that $f(t,b) \in \mathbb{N}$ for all real $t > T$.
- There is no proper (non empty) subset of A with the first two properties [18].

Attractors most commonly appear as geometric subsets of the phase space (points, lines, surfaces, etc.). Considered fleeting anomalies for some time, it has been demonstrated that more complex attractors exist too, manifesting into topologically wild sets that do not fit among the previously mentioned. When the attractor sets cannot be described as combinations of fundamental geometric objects, they are classified as *strange attractors*.

tory diverges from the equilibrium and approaches a large-amplitude spiking limit cycle (or some other attractor).

- *Supercritical Andronov-Hopf bifurcation.* The stable equilibrium loses stability and gives birth to a small-amplitude limit cycle attractor. As the magnitude of the injected current increases, the amplitude of the limit cycle increases too, so the trajectory becomes a full-size spiking limit cycle. The final situation is that of a stable limit cycle and an unstable equilibrium point.

Other than bifurcations of equilibria, bifurcations of limit cycle attractors are needed to complete this framework. These bifurcations typically correspond to transitions from repetitive spiking to resting behavior, and can be summarized in four categories, one of which is the already mentioned supercritical Andronov-Hopf, and a second is the saddle-node on invariant circle. Remaining bifurcations are fold limit cycle and saddle homoclinic orbit.

If we were to combine Saddle-node and Andronov-Hopf bifurcations of equilibria, along with fold limit cycle, homoclinic orbit bifurcation, and heteroclinic orbit bifurcation, we would describe thoroughly all possible bifurcations of codimension-1 on a plane.

It is interesting to notice that the *supercritical* and the *subcritical* Andronov-Hopf bifurcations cannot be simply viewed as temporal reversions of each other. In fact, in the case of the Supercritical bifurcation, we always have the system starting from or landing to a stable equilibrium point (or to a stable limit cycle together with an unstable equilibrium point). In the other case, the starting or arrival points are a single unstable equilibrium point, or an unstable limit cycle together with a stable equilibrium point.

This simple reasoning could already lead us to affirm that in the case of the FHN model with no delay, the system encounters a Supercritical Andronov-Hopf Bifurcation, since a stable limit cycle if formed starting from a stable equilibrium point. To support this statement with more rigorous elements, we need to add some details about Andronov-Hopf bifurcations (also known as Hopf bifurcations).

3.3.2 The Andronov-Hopf Bifurcation

To start with, the definition of the Hopf bifurcation for a system of ordinary differential equations is given. Let us consider a two dimensional autonomous system of ODEs

$$\dot{x}_1 = f_1(x_1, x_2, \alpha), \tag{3.19}$$

$$\dot{x}_2 = f_2(x_1, x_2, \alpha), \tag{3.20}$$

depending on a parameter $\alpha \in \mathbb{R}$, where f is smooth. Suppose that for all sufficiently small $|\alpha|$ the system has a family of equilibria $x^0(\alpha)$. Further assume that its Jacobian

matrix $A(\alpha) = f_x(x^0(\alpha), \alpha)$ has one pair of complex eigenvalues $\lambda_{1,2}(\alpha) = \mu(\alpha) \pm i\omega(\alpha)$ that becomes purely imaginary when $\alpha = 0$. Then, generically, as α crosses 0, the equilibrium changes stability and a unique limit cycle bifurcates from it. This bifurcation is codimension-1, as it needs only the $Re\ \lambda_{1,2} = 0$ condition.

Considering the differential equations system once again, it is possible to describe the bifurcation analytically. In particular, if the following non-degeneracy conditions hold:

- $l_1(0) \neq 0$, where $l_1(\alpha)$ is the first Lyapunov coefficient[3];
- $\mu'(0) \neq 0$,

then the system is topologically equivalent near the equilibrium to the normal form

$$\dot{y}_1 = \beta y_1 - y_2 + \sigma y_1(y_1^2 + y_2^2) \ , \tag{3.21}$$

$$\dot{y}_2 = y_1 + \beta y_2 + \sigma y_2(y_1^2 + y_2^2) \ , \tag{3.22}$$

where $y = (y_1, y_2)^T \in \mathbb{R}^2, \beta\ in\ \mathbb{R}$, and $\sigma = \text{sign} l_1(0) = \pm 1$.

- $= -1$, the normal form has an equilibrium at the origin, which is asymptotically stable for $\beta \leq 0$ (weakly at $\beta = 0$) and unstable for $\beta > 0$. Moreover, there is a unique and stable circular limit cycle that exists for $\beta > 0$ and has radius $\sqrt{\beta}$. This is a supercritical Andronov-Hopf bifurcation.
- If $\sigma = \pm 1$, the origin in the normal form is asymptotically stable for $\beta > 0$ and unstable for $\beta \geq 0$ (weakly at $\beta = 0$), while a unique and unstable limit cycle exists for $\beta < 0$. This is a subcritical Andronov-Hopf bifurcation [20].

In other words, the system undergoes a Hopf bifurcation when its eigenvalues cross the imaginary axis from the left plane to the right one. If the result of the crossing, in terms of a flow in phase space, is the transformation of a stable spiraling point in a limit cycle, then the bifurcation is supercritical. The subcritical case is usually more dramatic when experienced in applications. In this case the unstable limit cycle shrinks to zero, engulfing the stable fixed point and making it unstable. As α becomes positive after the bifurcation, every trajectory in the phase plane eventually ends on the stable limit cycle, being it the only attractor left.

In any case, the transition is governed by the variation of parameter α, which thus decides on the stability of the system. A simple example of the supercritical Hopf bifurcation can be observed[17] in the system

$$\dot{r} = \alpha r - r^3 \tag{3.23}$$

$$\dot{\theta} = \omega + br^2 \tag{3.24}$$

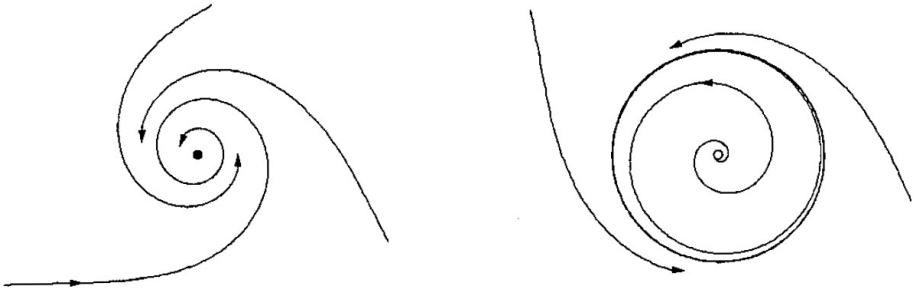

Figure 3.5: Dynamical behavior of the van der Pol oscillator in case $\alpha < 0$ (left) and $\alpha > 0$ (right). From S.H. Strogatz. *Nonlinear Dynamics and Chaos: With Applications to Physics, Biology, Chemistry, and Engineering.* CRC Press, 2015.

As shown in Figure 3.5, when $\alpha < 0$ the trajectories are spirals attracted to the fixed point in $r = 0$. When the sign of the parameter switches to positive values, a limit cycle appears. Trajectories drift away from the origin and approach the stable limit cycle. To check the mathematical validity of this dichotomy, we study how the eigenvalues behave when parameter α varies. The Jacobian of the system is computed, and we obtain $L = \begin{pmatrix} \alpha & -\omega \\ \omega & \alpha \end{pmatrix}$. The expression for its eigenvalues is easily computed and gives

$$\lambda = \alpha \pm i\omega \tag{3.25}$$

The obtained result matches the expectations, as the bifurcation point is found in correspondence of $\alpha = 0$. This model, however exemplifying it might be, carries some over-simplifications. In practical applications, the limit cycle is not circular most of the times. It is often elliptical, or it can have more creative shapes as in the FHN model case, in general, its shape depends on the value of α. Moreover, when the eigenvalues cross the imaginary axis, they do not follow a straight line, but rather a curvy path. This entails that there is a dependence of the eigenvalues to α.

3.3.3 Neurocomputational Properties

But where exactly does the bifurcation occur in our modelized neuron? The matter is not so simple as to determine a voltage or current defined threshold, above which the spiking response happens. As well discussed by Izhikevich in [13], although the notion of such an intuitive threshold is often employed by biologists, it is not always possible to find one. Or rather, it is not always meaningful to look for it, depending on the

[3]The first Lyapunov coefficient is a parameter-dependent function whose value at the critical parameter value contributes to determining the type of Hopf bifurcation that occurs. Its mathematical expression is computed in [19]

neurocomputational properties of the studied problem. Based on such properties, two main neuron categories are commonly identified, i.e., integrators and resonators.

For integrators, excitatory inputs push the state of the system toward the equilibrium attraction domain, and inhibitory inputs push it away. While in resonators, both excitation and inhibition push the state in the equilibrium point attraction domain, because such region wraps around the equilibrium and can be reached along any direction. This explains the presence of so called *rebound spikes*[4], which also generate some difficulty in defining a sharp threshold in resonators. One interesting difference, is that integrators present two possible membrane excitation configurations, and nothing in between. This behavior is regulated by the *all-or-none* law of physiology, that results in the distinction of curves corresponding to different values of external stimulus in two classes, the "all" and the "none" curves. As explained by Fitzhugh in his 1955 paper, "*within each class, the shapes of the curves vary continuously with z, but there are no intermediates between the members of the two classes*"[21], where z stands for the external stimulus in his notation. The threshold phenomenon marks the separation between those classes, and can be visualized picturing a common curve parting in two different curves at a certain time between zero and the time corresponding to the peak of the "all" spike, when it is clear that the depolarization has taken place. The case of resonators, on the other hand, is not so clear-cut. Resonators can generate spikes of an intermediate amplitude, neither "all" nor "none", when the state is pushed between postsynaptic potentials trajectories and spike trajectories. This explains the observation of partial-amplitude spiking, even though it is quite difficult to detect, since the voltage range that allows such behavior is typically very thin.

Summing up, *integrators have well-defined thresholds; resonators may not*[13]. Moreover, if thresholds are defined, they are described not by numbers but by manifolds which separate different regions of the phase space, behaving like *separatrices* of the phase plane. Many resonators, including the Hodgkin-Huxley model, have *quasi-thresholds* instead of thresholds, thus permitting all intermediates between "all" and "none" responses. The width of the quasi-threshold in the Hodgkin-Huxley model is so narrow (it can be as small as $0.0001mV$) that it appears to be smaller than membrane potential noise fluctuations. For all practical reasons, it may be assumed to be just a curve.

One more difference between the two types of neurons is that integrators prefer high-frequency inputs, the higher the frequency, the sooner they fire, since it all comes down to increasing the membrane potential. The case is different for resonators. The response of the resonator depends on the frequency content of the input, thus, the effect of the second impulse depends on its timing. Whether it kicks in when the trajectory is half-way, or if it has completed a full cycle, it will cancel out or add to the first input, respectively.

[4]Spikes that come in response to a brief hyperpolarizing pulse.

3.4 External Stimulus: the No Delay Case

In the formulation proposed by equations 3.16 and 3.17, u is the fast variable, it presents a *quasi-threshold* spiking dynamics, mimicking the membrane potential. Conversely, the slow variable v is a recovery variable, it represents the characteristic refractoriness of neurons after firing. The separation between the mentioned time scales is dictated by the factor ε. This marked difference causes the stiffness of the equations system. $I_{ext}(t)$ is the external stimulus, in this case it is described by a time-dependent function which can be a rectangular wave, a delta kick or any other kind of delta-like function, possibly representing currents given by the interactions with other neurons, or by external stimuli. Finally, a is a dynamical parameter regulating the dynamical regime of the model.

The nullclines of the model have a cubic form in equation's 3.16 case, while the second nullcline is a vertical line:

$$v = u - \frac{u^3}{3} + I_{ext} \tag{3.26}$$

$$0 = u + a \tag{3.27}$$

These lines intersect in one point only, whose positions depends on parameter a, on the shape of the cubic nullcline, and on the magnitude of I_{ext}. Let us determine how the stability of a generic $(u*, w*)$ equilibrium point depends on the mentioned factors.

The Jacobian matrix of the FHN model at the generic equilibrium point $(u*, w*)$, obtained through linearization of the differential equations system, has the form

$$L = \frac{1}{\varepsilon}\begin{pmatrix} 1 - u^{*2} & -1 \\ \varepsilon^{-1} & 0 \end{pmatrix} \tag{3.28}$$

The trace Tr and determinant Δ of the Jacobian matrix are computed to determine the stability of the system.

$$Tr = \frac{1 - u^{*2}}{\varepsilon} \quad \text{and} \quad \Delta = \frac{1}{\varepsilon} \tag{3.29}$$

For the system to be stable, both eigenvalues need to be negative. This translates to conditions $Tr < 0$ and $\Delta > 0$, where the former is always verified. It is simple to explicitly compute the only equilibrium point, since it is given by the only possible intersection of the nullclines: $(-a, a - \frac{a^3}{3})$. Substituting this point in the Jacobian's trace and determinant equations, it is obtained that the system becomes unstable when $|a| < 1$, and is stable otherwise. In this model, a is thus the only parameter playing a role in the system stability. In fact, when $|a| < 1$ the system undergoes a supercritical Hopf Bifurcation and a stable limit cycle appears.

The system, as we now show, behaves somewhat similarly to the fore-mentioned van der Pol equation. Let us suppose that the system is found in a point in phase space close

to equilibrium. Giving external impulse though I_{ext}, depending on the signal amplitude, will give rise to different situations.

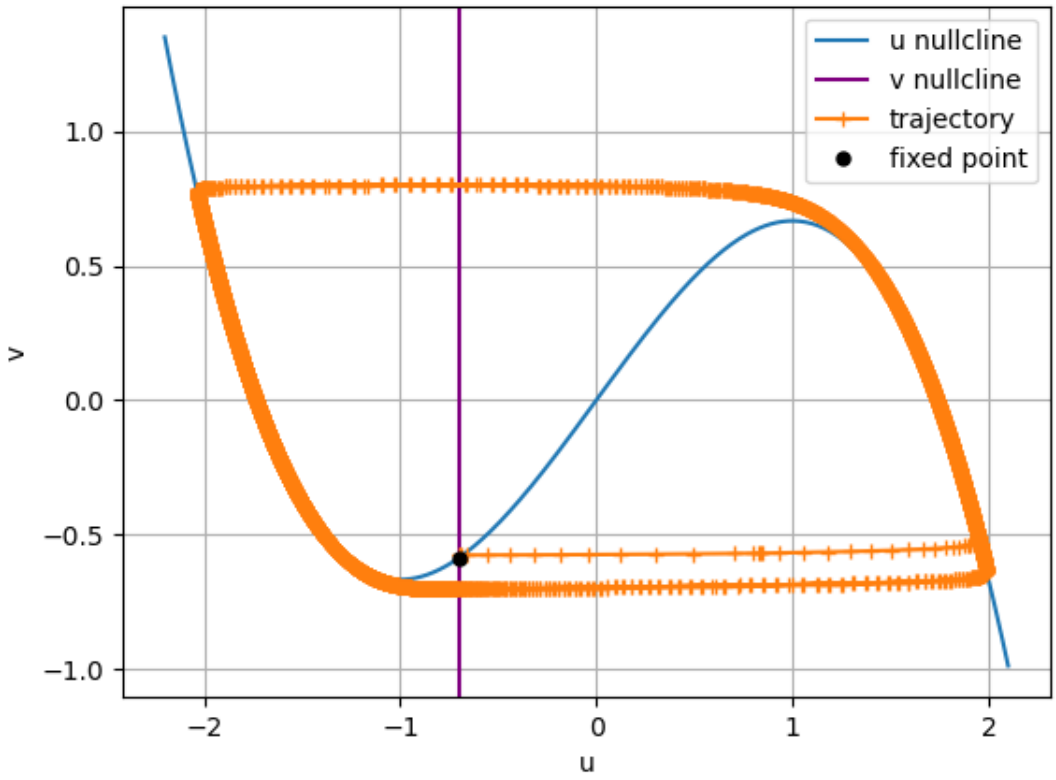

Figure 3.6: Phase plane of the non-delayed system in the limit cycle state. In these conditions, the limit cycle is an attractor for all trajectories in the phase plane, and the fixed point becomes unstable.

In the first case the given impulse is sub-threshold, which means that the dynamics is spatially limited around the equilibrium point, the trajectory rapidly spirals around the equilibrium point before collapsing onto it. Intermediate stimuli result in intermediate-amplitude trajectories that correspond to partial-amplitude spikes. This is the manifestation of the absence of all-or-none spikes. This situation is numerically rather difficult to obtain. It is verified in the case of the considered phase point being set exactly to be on the middle branch of the cubic nullcline. Indeed, when evaluating the stability of the system in that area of the phase space, we find that any point close to the middle branch is strongly repelled away from it. This kind of computation had been carried on by FitzHugh himself. Given the difficulties of setting an exact value for x, and the unavoidable noise associated with numerical integration, it was practically impossible with

the computational power of the time to actually follow along the middle branch and thus obtain the intermediate behaviour. Therefore, FitzHugh assumed that the system would exhibit virtually only the all-or-none behavior. We will follow along this decision, thus considering that the threshold set can be treated as a simple threshold manifold without committing too big of an error. In the last case, the impulse is big enough to generate a wider dynamics. This condition will result in the destabilization of the equilibrium point, and in the formation of a limit cycle. In other terms, this translates to the tonic spiking neuron behavior.

To give sounder basis to the dynamics of the system, we can take advantage of the widely different time scales of the system. The presence of factor ε determines a motion of order 1 for the v variable, and of order ε for the u variable. In particular, considering the small magnitude of ε, if we consider only the u dynamics, it is reasonable to assume v as equal to a fixed value $\bar{v}$.

In that case, the dynamics equation becomes

$$\varepsilon \dot{u} = u - \frac{u^3}{3} - \bar{v} \tag{3.30}$$

which exhibits different stability depending on the value $\bar{v}$ assumes. If $|\bar{v}| < \frac{2}{3}$ the phase space presents two stable equilibrium points and a central unstable one. This situation is shown in Figure 3.7. In the case of $|\bar{v}|$ being exactly equal to $\frac{2}{3}$, we have a limit situation, presenting a saddle point together with a stable equilibrium point. In the remaining case, shown in Figure 3.8, the phase space exhibits a single stable equilibrium point. By making a dynamical analysis of this simplified situation, it is possible to gain some intuition on the generation of the spike in the neuron.

Let us first consider the case $|\bar{v}| < 2/3$. The displacement of the system happens on the horizontal line crossing $\bar{v}$, and it is proportional to the magnitude of the initial impulse, which in the simulations we took to be a Dirac delta distribution. Once the shock is applied in the positive u direction, if the trajectory does not pass the unstable middle equilibrium point, then the system is repelled back to the stable point. If the impulse is enough for the trajectory to go beyond the unstable point, then the system becomes attracted to the second stable point, thus traveling across the u nullcline and landing on the right-hand branch [10].

We might visualize this by imagining that the phase point, once it has reached the minimum of the u nullcline through the external impulse, falls off from it, and rapidly travels to the opposite branch. Dynamically, the outer branches of the cubic nullcline are attractive, while the middle branch is strongly repulsive. In the original paper by FitzHugh, the area around the nullcline middle branch was in fact ironically but aptly called “no man’s land” for this reason, as can be seen in Figure 3.4.

From the landing point onward, the motion is governed by the dynamics of time scale-1, that approximately follows along the right branch, and could be described by

the equation

$$v = u - \frac{u^3}{3}. \tag{3.31}$$

The same behavior is observed once the phase point arrives around the maximum of the u nullcline, which it leaves abruptly to almost-horizontally travel to the left branch, as shown in Figure B.1.

Once the phase point has landed back on the cubic nullcline, the dynamics of time scale-1 resumes. If the magnitude of the initial voltage kick is sufficient, this cyclic motion is repeated indefinitely, i.e., the limit cycle is formed.

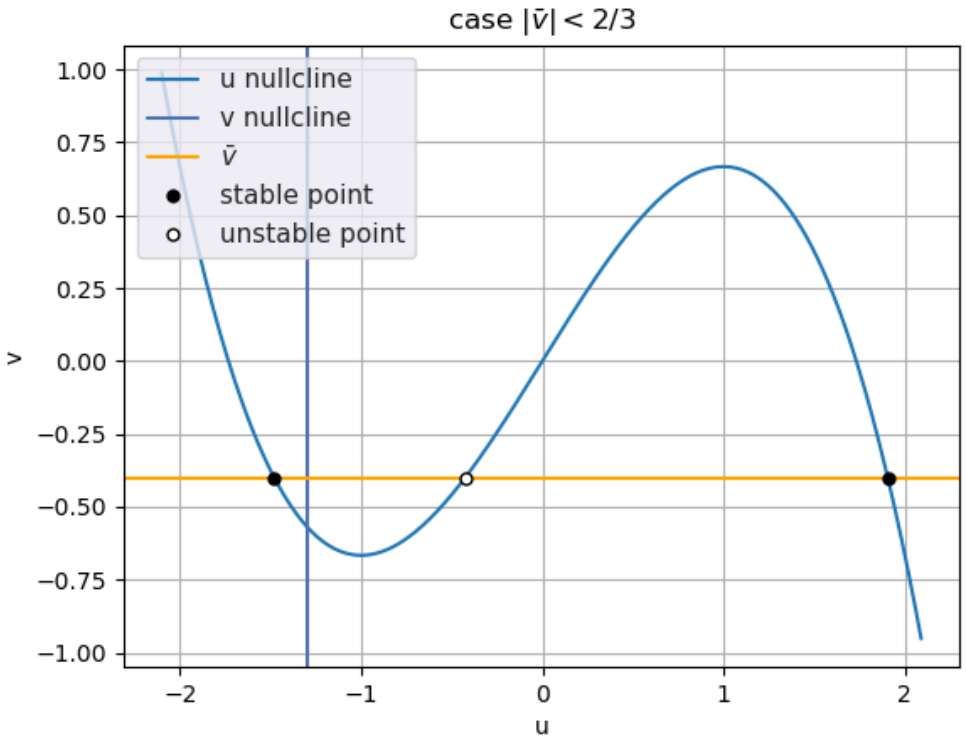

Figure 3.7: Nullclines and equilibria in the $|\bar{v}| < 2/3$ case. The systems displays two stable and one unstable equilibrium points.

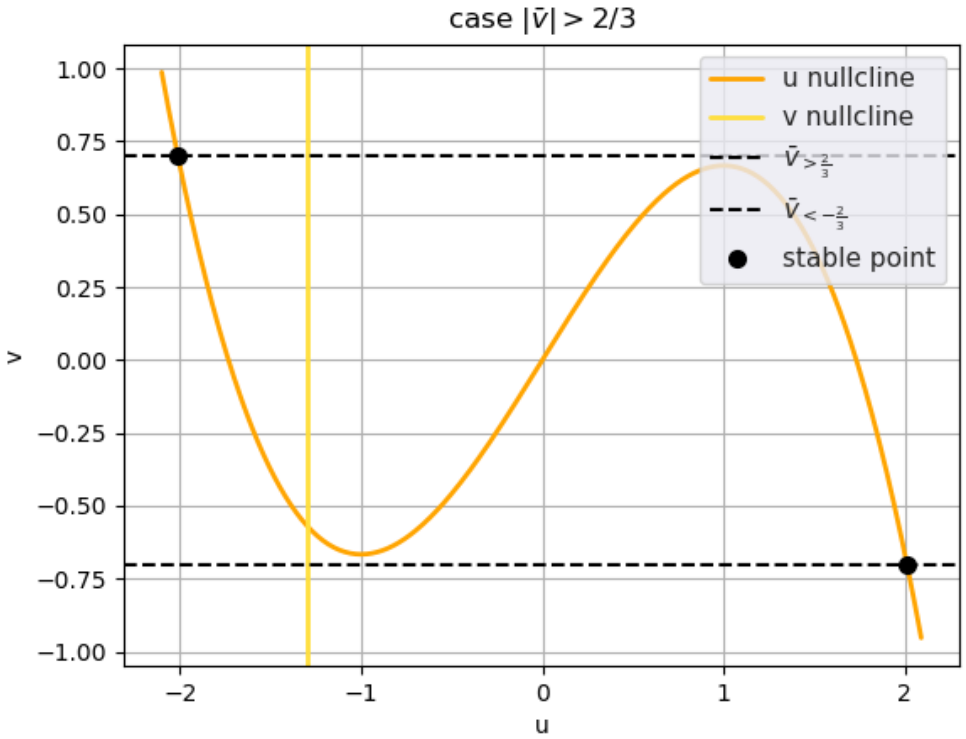

Figure 3.8: Nullclines and equilibria in the $|\bar{v}| > 2/3$ case. The systems displays one single stable equilibrium point.

Chapter 4

Feedback phenomena: Self-Coupled Delay Term in the FHN model

The introduction of the delay term shown in 3.18 allows a more physical description of the simplified neuron system. As seen in Chapter 2, the modelization of the neuron can become more realistic by taking into account impulse transmission times in axons and synapses. This is commonly done by introducing a delay term in the differential equations describing the dynamics of the system. In this case, the delay term does not represent the coupling of different neurons, instead, it represents a stimulus produced by the system itself to try and sustain itself without the need of an external input, so it is a self-coupled term. As already seen, the term at issue is simply given by the activation variable u computed at a time prior to the one considered in the left-hand side of the equation t, minus $u(t)$, all multiplied by a constant representing the strength of the "coupling" among system elements, in this case, between past and present state. The term $u(t-\tau)$ thus introduces a reference to a past dynamical state, and turns the system of equations in the DDEs system

$$\dot{u}(t) = u(t) - \frac{u^3(t)}{3} - v(t) + J(u(t-\tau) - u(t)) \tag{4.1}$$

$$\dot{v}(t) = u(t) + a \tag{4.2}$$

A similar problem has already been studied in [22], where the delay is introduced to simulate the phenomenon of recurrent neural feedback. When the impulse is given as feedback by another cell, or by the cell itself, in our case, the injection of current is not immediate due to non-zero conduction time and to synaptic delay. The simplest way to modify the non-delayed model is thus to introduce the delay term 3.18. It is important to assign moderate values to J and τ, and in particular τ should not be too small, because the combined synaptic delays and conduction times of the system are greater than the duration of a single action potential.

The presence of delay, adds up to the complexity of the system, being non-linear already, so the problem presents a series of features and behaviors that are not quite immediate to locate and explain. Similarly to the non-delayed problem, the FHN model with delay also exhibits, at the variation of the parameters, the double behavior: small dynamics close to the equilibrium point (resting state), and tonic spiking state.

The two models, however, are different in more than one way, from a dynamical point of view. First off, it is important to notice that in the simpler case with no delay, there is a qualitative transition in the dynamical framework. As shown in chapter 3, the system undergoes a supercritical Hopf bifurcation: the stable point becomes unstable, and the limit cycle appears. When the limit cycle is formed, the unstable point, found at the crossing of the nullclines, remains inside the cycle, as can be clearly seen in Figure 3.6.

In the DDE case, the situation is quite different. Some simulations were performed considering parameters variations is relatively broad ranges. In all the explored parameters configurations, we see that the limit cycle is formed above the crossing point of nullclines, leaving the initial point outside of the closed structure, as shown in Figure 4.1. Moreover, if we were to study the linearized system, we would discover that no supercritical Hopf bifurcation occurs. The stable point does not lose stability, which means that in the limit cycle configuration two attractive structures coexist [23].

To grasp other aspects of the system behavior we performed some simulations using the numerical integrator RADAR5, later presented in Appendix A. In the following, we will present some of the results obtained during the simulations.

4.1 Variation of Integration Parameters: an Overview

Some simulations were performed varying all parameters in defined ranges, to gain an idea of the general response of the system to such variations. Considering the non-linearity of the system and the additional complexity given by feedback, it was not possible for the scope of this work to give full analytical interpretation of all phenomena. As will be furthered in Appendix B, if the integration is performed with the RADAR5 integrator, it is possible to consider the singular case $\varepsilon = 0$. From a dynamical point of view, in the $\varepsilon = 0$ case, the first equation of the system is "infinitely" fast, since the right-hand side of the equation tends to infinity for $\varepsilon \to 0$. The limit cycle is still produced in the right parameter configuration, but it presents some differences compared to the one obtained with moderate ε values. The transition from the motion along one branch of the cubic nullcline to the opposite side branch becomes extremely sharp. The jump becomes nearly rectilinear, with a sharp angle instead of the curve observed in $\varepsilon >> 0$ cases. The shape of the spike becomes more "geometrical", losing its smoothness. The possible dynamical configurations of the system, meaning the presence of the tonic spiking and of the resting

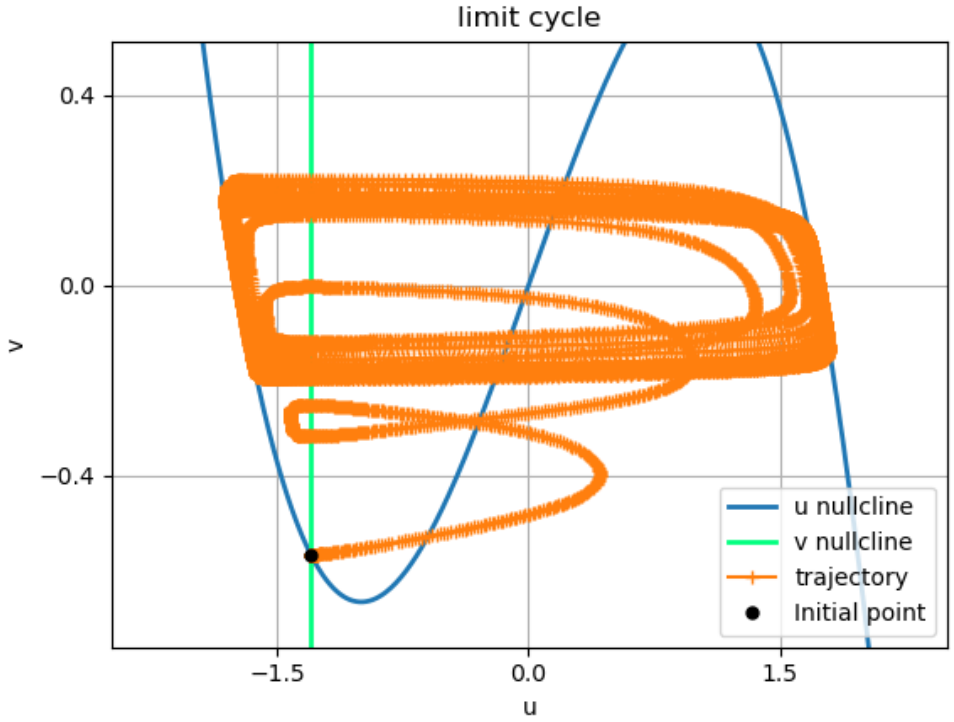

Figure 4.1: Limit cycle for the system with time delay. Initialization parameters are set to $\varepsilon = 0.01$, $a = 1.3$, $J = 1.5$, $\tau = 1.0$. Two more parameters, amplitude and standard deviation, are needed to initialize the external Gaussian impulse in the numerical integrator. Here $amplitude = 0.2$, $\sigma = 0.1$

phase, remains unvaried. There is however a variation in the quasi-threshold position, since the point where the transition between the two phases happens does not stay the same, considering the same parameter configuration.

4.1.1 Joint variation of J and τ

One interesting subject is the individuation of the quasi-threshold manifold position with the variation of integration parameters. We have already mentioned the effect produced by the variation of ε. Given the focus of this Chapter, it is relevant to study how changing the parameters of the self-coupled delay term affects the behavior of the system. In particular, we performed a simulation that involves the independent variation of parameters J, the coupling constant, and τ, the time delay value.

The results are shown in Figure 4.2. In case the system reaches the spiking state, it is possible to numerically compute the asymptotic value of the limit cycle area. Those

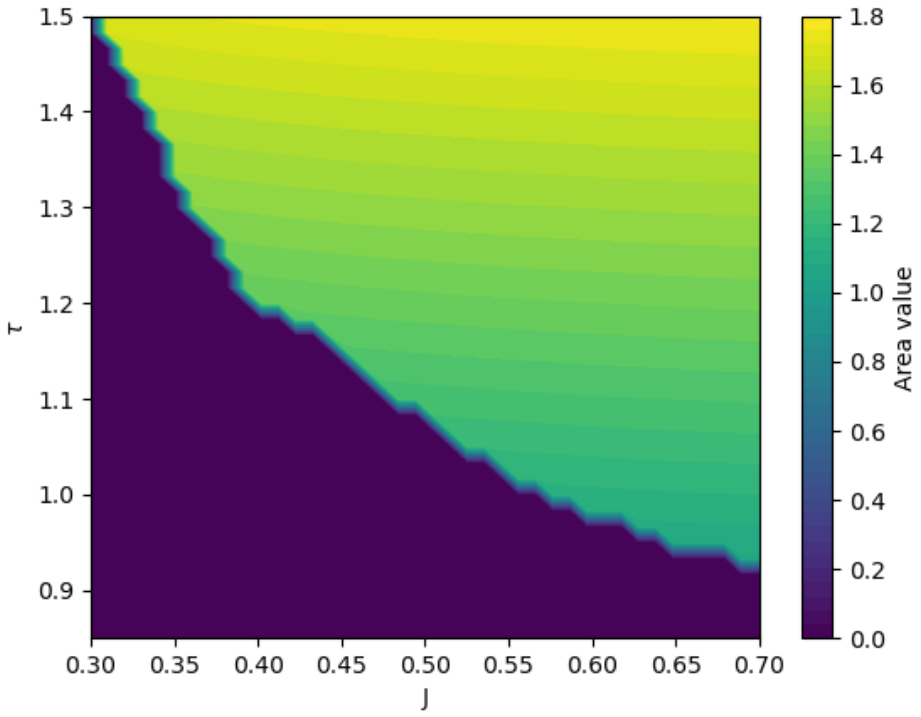

Figure 4.2: Computed area values with dependence to the variation of J and τ. Areas equal to 0 correspond to a damped phase in the system, no limit cycle is formed and since trajectories spiral to the stable equilibrium point. In the other cases, the system is in the limit cycle phase. Depending on parameter values, areas might differ slightly, varying in a range from 1.0 to 1.8 measure units approximately.

cases are represented by green-yellow colored markers. Dynamically, there are two more possibilities. The areas associated to a 0 value, correspond to the system spiraling around the equilibrium point after the initial kick, and eventually collapsing back to the resting state, the damped case. The remaining case, corresponds to the over-damped case. In such situations, the system follows along the nullcline tracing a wide trajectory, but never crosses the v nullcline.

4.2 Considerations on the Delay Term

The main question that we tried to answer to through the simulations is that of how the FHN system's behavior changes once feedback is taken into account. In general, we might say that the system tries to stabilize itself in a self-sustained dynamics made possible by the presence of the feedback term $J(u(t) - u(t - \tau))$.

The first result concerns the study of the delayed component. To start the simulation, a voltage "kick" is necessary the to correctly initialize the impulse, which in a first moment is supplied externally. The starting point is thus that of a wave-like Gaussian impulse hitting on the neuron structure. Because of the intrinsic nature of the system, the stimulus only initially comes externally, and is thereafter generated by a feedback phenomenon, in turn produced by the delay term.

The impulse produced by delay does not maintain its Gauss shape for the whole duration of the simulation. It actually gains a peculiar shape almost immediately after the starting point. The depiction of the feedback impulse is shown in Figure 4.3, in a spiking state configuration of the system.

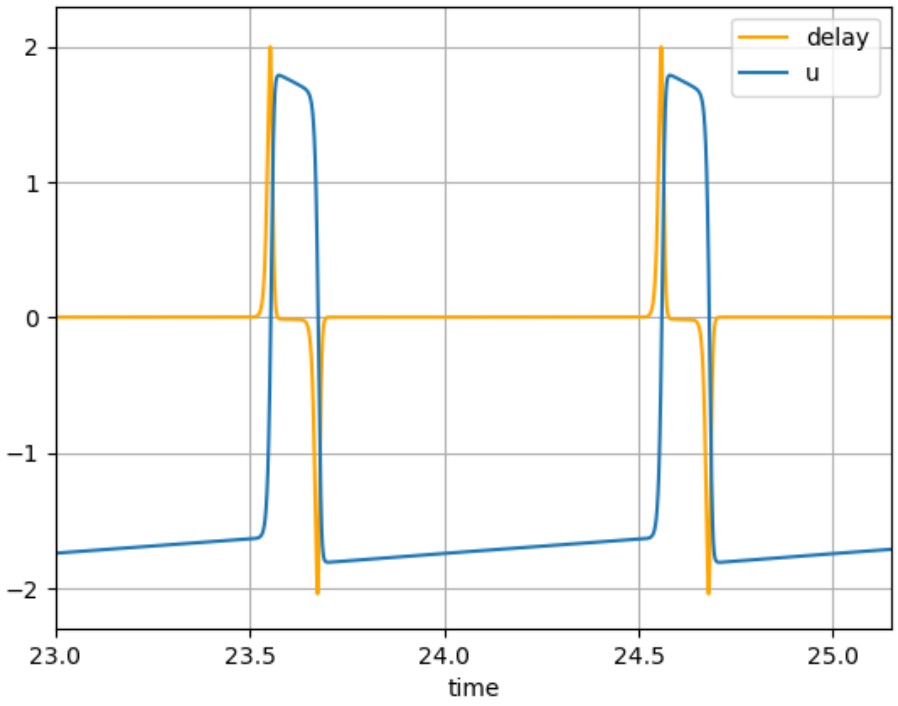

Figure 4.3: Self-coupled term plotted over u. The spiking variable u is generated by feedback response of the system. In this simulation parameters are set to $\tau = 1$, $\varepsilon = 0.01$, $a = 0.7$. The external kick is given by a rectangular impulse 0.01 time units wide.

As we can notice from the picture, the feedback impulse exhibits a double bulge. The first, above zero, comes immediately before the spike, the second is negative, and follows the spike. The effect that the shape of the feedback impulse has on the system is easily interpretable. Since the system is in the tonic spiking phase, the first bulge is generated by the system to sustain the limit cycle. The second bulge produces the inhibitory phase

of the simulated neuron, forcing the system to come down from the spike and make itself available to undergo a new spike at the following cycle.

Since the feedback pulse comes directly from $u(t) - u(t - \tau)$, it is clear that if the system was to replicate itself identically at each τ, the feedback would immediately become zero. This in turn would imply that there would be no external source to sustain the system, and thus we would not see the periodic spiking. It appears indeed that the spikes rise from ground-level voltage a small amount of time later at each τ cycle. The total delay after a 20τ spiking period is around 0.1 time units. This is enough for the system to generate a sufficient feedback impulse, and thus to keep the spiking alive.

4.3 Areas Trend in a Spiking State Configuration

To better understand the behavior of the system when undertaking the limit cycle, we resorted to a variation of *Poincaré maps*, mathematical tools employed in the field of dynamical systems. Poincaré maps, or first recurrence maps, keep track of the intersection of periodic orbit in the state space of a continuous dynamical system with a certain lower-dimensional subspace, called *Poincaré section*, transversal to the flow of the system. The periodic orbit is clearly represented by the system's limit cycle in this work. As for the Poincaré section, it was necessary to identify a bi-dimensional subset that could be a good fit to comprehend both the spiking state and the resting state phases. With this target in mind, we chose to consider the negative half line of the v nullcline, which is necessarily crossed both by limit cycles and limited dynamics. Theoretically, one's aim would be to obtain the distribution of the points at which the periodic orbit crosses the Poincaré section, and extract some conclusions from it. Our approach in this work was slightly different, because the interesting information is rather how the area of the limit cycle (or the "generalized area" of the resting state phase) varies between each crossing of the Poincaré section.

The first analysis concerned generalized areas. The term generalized is used because no actual closed shape is formed in the phase plane in this configuration. There are two possible cases where this happens, the first happens in correspondence to an over-damped behavior of the system. In that case the system receives a considerable initial kick and travels the cubic nullcline on a wide trajectory, only once. The trajectory ends with an asymptotic approach of the equilibrium point, but the v nullcline is never actually crossed. The second case, instead, is damped. The trajectory travels around the nullcline for a short time period, and then rapidly goes back to the equilibrium point. Since in this configuration the system does not dwell much before spiraling onto the stable point, the analysis was performed on a few points only. It is not very meaningful, considering the small sample, to extract reasonable conclusions, it can be however be reported that the trend seemed to indicate an exponentially increasing speed in the collapsing dynamics.

In the second part we performed some tests on the limit cycle areas computation. It was necessary to cut off the transient period, during which the system is in the process of landing on the stable limit cycle. When the system lands in the spiking state, it is possible to compute limit cycle areas and make some considerations on the results. First of all, we know from the theory that a stable limit cycle is reached at some time t^*, so it was expected to find some speed trend of the areas $A(t)$ approaching the final $A(t^*)$. One hypothesis was that the areas should reach the asymptote exponentially fast, similarly to the case of the stable equilibrium phase. In other words, we hypothesized that the areas obeyed a law of the following kind:

$$A(t) = a - b\exp(-ct) \tag{4.3}$$

With $a, b, c > 0$. A fit was performed both on the function $A(t)$ and on its total time derivative $\frac{dA}{dt}$. From the double analysis we obtained two independent estimates of the parameters (only b and c in the second case since the a term disappears in the derivative) that matched well, possibly confirming the exponential trend supposition. The graphical representation of the results are presented in Figure 4.4 and Figure 4.5.

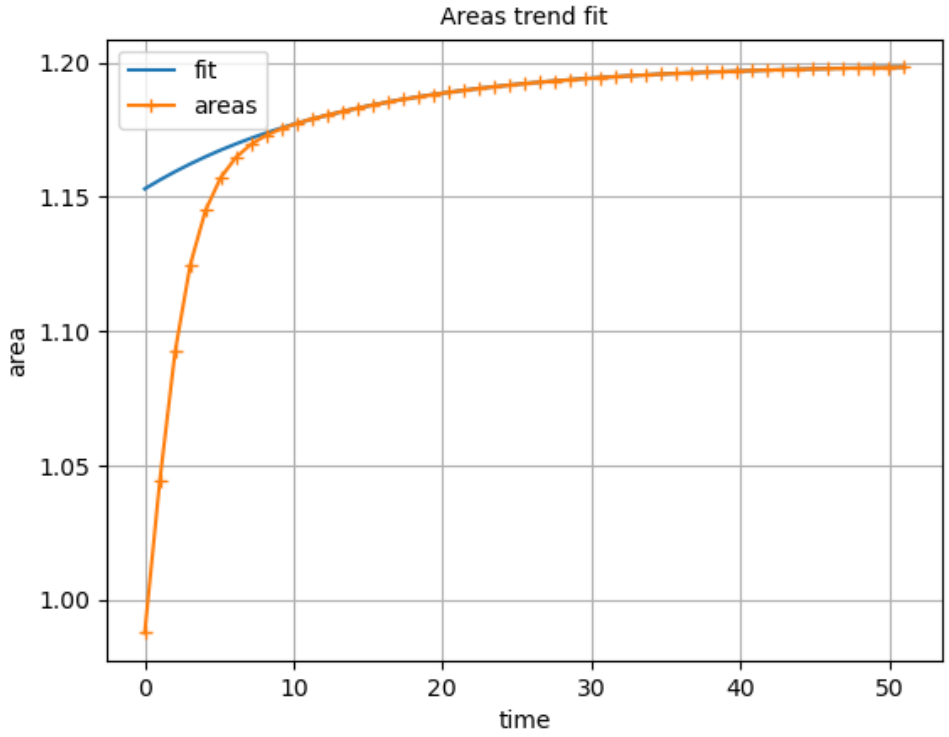

Figure 4.4: $A(t)$ trend and relative fit. The searched fit function is $A(t) = a - b\exp(-ct)$.

The fit process, performed with the `curve_fit` function from the `scipy.optimize` Python library, returned the following values for a, b and c parameters and their standard deviation errors:

a	1.199346± 0.000007
b	0.046356 ± 0.000033
c	0.073103 ± 0.000069

Table 4.1: a, b and c parameters obtained via exponential fit of the function of limit cycle areas in time.

b	0.0458 ± 0.0001
c	0.0738 ± 0.0001

Table 4.2: b and c parameters obtained by fitting the linearized function of limit cycle areas with respect to time.

In this case the fit was obtained through the `linregress` function from the `scipy.stats` Python library. It was possible to obtain estimates for parameters b and c and their standard deviation errors:

The obtained data is relatively well matching, indicating that the proposed hypothesis is likely to be correct.

These results entail that when the system enters the spiking phase, with the repetition of an infinite number of successive limit cycles, cycle areas start to approach an asymptotic value. With the parameters set to be as presented in the table, the limiting areas was found to be equal to 1.1993 units. The time derivative of the areas trend is exponential, indicating that the asymptote is reached exponentially fast.

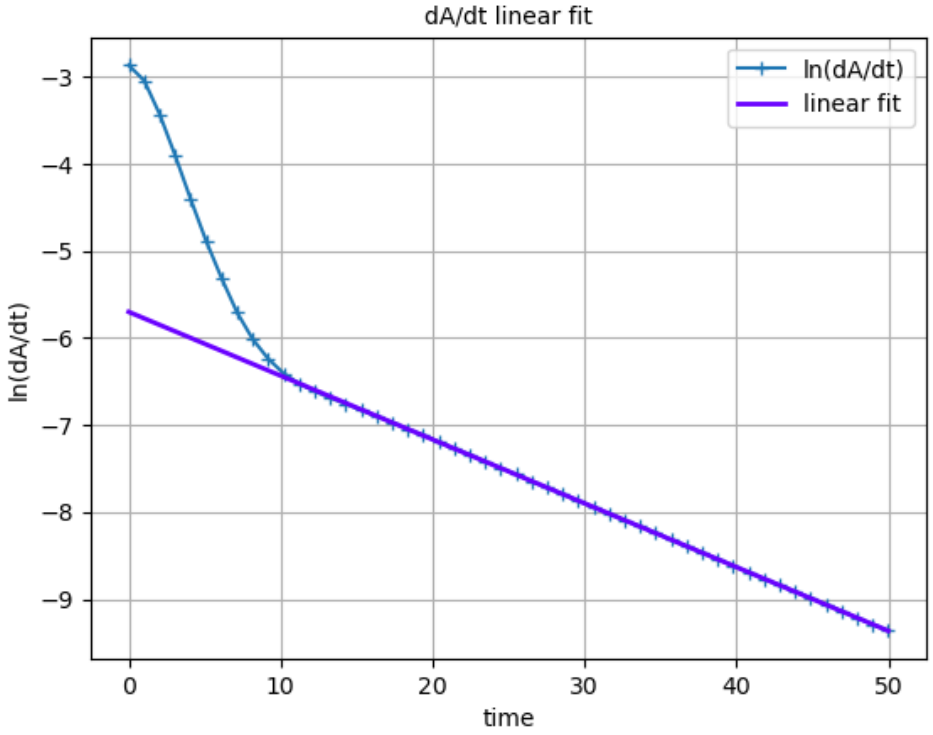

Figure 4.5: The time derivative of function $A(t)$ has an hypothesized negative exponential trend, given by $\frac{dA(t)}{dt} = bc\exp(-ct)$. To perform the fit, the natural logarithm of the differentiated data has been considered, so to obtain linearly distributed points.

Chapter 5

Conlusions

In this dissertation, we have considered the FitzHugh-Nagumo dynamical model of the neuron, deepening some of its relevant aspects in the framework of dynamical systems theory. We initially studied a variation on the original system comparing its dynamical features to those of the van der Pol equations. More than one similarity was found between our system and the relaxation-oscillator, we proceeded by analogy in the identification of some aspects of the system. Fundamental themes such as equilibrium, stability, limit cycle attractors and the theory of bifurcations have been deepened, with a view to the interpretation of the FHN system's behavior.

The focus of this work lays on the research towards a more realistic description of the behavior of the single excitable cell as part of an ensemble of interacting neurons thus for example considering conduction times between different neurons. This aspect has been explored on a single neuron via introduction of a self-coupling term with delay in the differential equations system. The presence of time delay in dynamical systems determines an enrichment in terms of dynamical features of the system, other than making the model more applicable and predictive. Some of the analysis carried out in this dissertation could be reinterpreted and employed in works that focus on neural systems and networks of neurons.

Given the complex analytical form of the differential equations system in presence of a time delay term, the considerations on this topic have been developed in a simulation-based fancy. Such simulations are mainly apt to broaden the understanding of how the behavior of the system changes compared to the non-delayed version, thus to acquire knowledge on feedback phenomena and medium field systems of neurons.

The differential equations system featured the presence of several parameters, some having an influence on its dynamical behavior. We studied how varying them in ranges established in advance would change the phase plane picture of the system. One point of interest is that of the presence of a semi-threshold which differentiates two dynamical phases of the system: the tonic spiking and the resting phase. From a dynamical point

of view, these two phases correspond to the presence of a stable limit cycle in the phase plane in the former, and of a stable focus in the latter. It is relevant to notice that this transition does not entail the presence of a Hopf bifurcation, which instead was met in the non-delayed case. Some effort was spent on determining where the quasi-threshold is met in different parameters conditions, in particular, we studied the results of varying the self-coupling delay term in terms of identification of three different dynamical states. These are the formation of the limit cycle, with slightly varying asymptote areas depending on parameters choices; a damped phase in which trajectories spiral around the stable fixed point before settling in a static state; an over-damped phase that features the system traveling the cubic nullcline in a wide trajectory, eventually asymptotically approaching the equilibrium point.

Given the peculiar features the system acquires in the presence of a delay term, we chose to deepen the subject of the delay term. Following the definition of such term, given by $J(u(t) - u(t - \tau))$, we extracted simulated data and were able to plot the feedback term itself. We found that the feedback stimulus presents a rather periodic behavior, its shape is quite easily interpretable knowing the system response.

When in the tonic spiking phase, the system forms a stable limit cycle in the phase plane which is traveled periodically. We studied how the limit cycle area varied at each iteration, hypothesizing that the trend should present an asymptote which ought to be reached exponentially fast. By performing two independent fit tests on the trend of the areas and of their time derivative, such claim proved to be compatible with the obtained results. These tests were performed following the prescriptions of the Poincaré map theoretical framework, however with some adaptations needed by the specific context. Numerical results on the determination of the asymptotic area in a specific parameters configuration can be found in Chapter 4.

Appendix A

Stiffness

Stiffness is a subtle but important concept in the numerical solution of differential equations. In general, we could say that a differential equation problem is stiff if it has a slowly varying solution, but at the same time there are other solutions that vary rapidly. This forces most numerical methods to take small steps to obtain satisfactory results, and thus it entails high computational costs.

Some numerical tools have been developed to confront this issue. The methods with the highest efficiency for stiff problems are implicit methods. An overview of these methods is given in Appendix B. The main idea with using implicit methods, is that they allow the user to take bigger integration steps, but do more work for the single step. Since the main concern with the integration of stiff equations is about efficiency, being able to increase the step size is crucial [24].

Although it is not easy to give a universal definition of systems stiffness, some attempts have been done. For linear systems, the custom is to compute the eigenvalues of the system and compare their relative magnitudes. If widely different magnitude scales are found, the system is highly likely to be stiff. A commonly used stiffness index, assuming that $Re(\lambda_i) < 0$ for all system eigenvalues λ_i is

$$L = max|Re(\lambda_i)| \tag{A.1}$$

, where it is important to notice that L is not invariant under the rescaling of the system. Such rescaling must in fact be accompanied by a change of error tolerances, which play a central role in the evaluation of the possible stiffness of the system.

The measure used for linear systems is extended to general differential equations by considering eigenvalues of the local Jacobian matrix. Pure imaginary eigenvalues are not allowed in these measures of stiffness, because problems with high frequency oscillations require a completely different approach. Another measure of stiffness can be given by

$$S = \frac{max|Re(\lambda_i)|}{min|Re(\lambda_i)|}. \tag{A.2}$$

If we were to accept the reasoning behind this index, then the system could be considered to be stiff if the stiffness index was found to be large. Nevertheless, to be more specific, the relevant term in the evaluation of the system's stiffness is not only the magnitude of L, since the time interval where the index is evaluated must be considered as well. In simple terms, if L is large but the time interval of evaluation is extremely small, as it happens in some models, then the problem might be solved with explicit methods, thus it cannot be labeled as stiff.

One more difficulty that arises in case of stiff systems is that of computational stability. When combining the need to obtain accurate solutions and at the same time keep the computation stable, the latter forces to reduce greatly the magnitude of the steps. This is generally not necessary for non-stiff problems.

To wrap these concepts up, we might use Shampine and Thompson's words that "*whether an initial value problem is stiff depends on the stability of the problem, the length of the interval of integration, the stability of the numerical method, and the manner in which the method is implemented*". [25] Often, the best way to know if a method is stiff or not is to simply try our hand at the integration with explicit methods. If the solution is not satisfactory, the problem may be stiff.

Appendix B

Numerical Integration

As already pointed out, one of the critical issues in the handling of DDEs and in particular of stiff equations, is their integration. The software has improved greatly through the years, although it is not yet as advanced as the one employed in ordinary differential equations problems.

The approach followed by many DDE solvers is to use explicit Runge-Kutta methods to integrate the differential equations system. Explicit methods, however, are not suitable for the integration of stiff problem, these are in fact often handled with implicit methods. For sake of completeness, we will give a brief overview of both.

Runge-Kutta methods are a family of iterative methods developed more than a century ago by mathematicians Carl Runge and Wilhelm Kutta. Their most common application takes place in the field of ODEs, where the initial value problem can be specified as:

$$\frac{d\mathbf{y}}{dt} = f(t, \mathbf{y}), \quad \mathbf{y}(t_0) = \mathbf{y}_0 \tag{B.1}$$

Here y is an unknown function of time t. The aim of the integration methods is to find the approximate solution of y starting from the stated problem. In the classic Runge-Kutta method, commonly known as RK4, an integration step-size $h > 0$ is picked, and the following are defined, as in [26]:

$$\mathbf{y}_{n+1} = \mathbf{y}_n + \frac{1}{6}(\mathbf{k}_1 + 2\mathbf{k}_2 + 2\mathbf{k}_3 + \mathbf{k}_4)h, \tag{B.2}$$

$$t_{n+1} = t_n + h \tag{B.3}$$

for $n = 0, 1, 2, 3, ...$, using

$$\mathbf{k}_1 = f(t_n, \mathbf{y}_n) \tag{B.4}$$

$$\mathbf{k}_2 = f(t_n + \frac{h}{2}, \mathbf{y}_n + h\frac{\mathbf{k}_2}{2}) \tag{B.5}$$

$$\mathbf{k}_3 = f(t_n + \frac{h}{2}, \mathbf{y}_n + h\frac{\mathbf{k}_1}{2}) \tag{B.6}$$

$$\mathbf{k}_4 = f(t_n + h, \mathbf{y}_n + h\mathbf{k}_3) \tag{B.7}$$

The local truncation error in the RK4 method is of order $O(h^5)$, while the total accumulated error is of $O(h^4)$ order. This condition is referred to by stating that the RK4 is a fourth-order method.

The Euler method is a well known member of the Runge-Kutta family, while still being useful for many applications, it is only first-order accurate, i.e., the function f needs to be evaluated a single time. More advanced Runge-Kutta methods aim to achieve higher accuracy by sacrificing the accuracy of Euler's method through the re-evaluation of $f(.,.)$ at points intermediate between the previously adjacent points $(\mathbf{x}_n, \mathbf{y}(\mathbf{x}_n))$ and $(\mathbf{x}_{n+1}, \mathbf{y}(\mathbf{x}_{n+1}))$.

Explicit methods are a generalization of the example given above:

$$\mathbf{y}_{n+1} = \mathbf{y}_n + h\sum_{i=1}^{s} b_i k_i, \tag{B.8}$$

where $\mathbf{k}_i$ have generalized expressions as well. We display a generic coefficient expression for clarity:

$$\mathbf{k}_j = f(t_n + c_j h, \mathbf{y}_n + h(a_{j1}\mathbf{k}_1 + a_{j2}\mathbf{k}_2 + ... + a_{j,j-1}\mathbf{k}_{j-1}). \tag{B.9}$$

Implicit Runge-Kutta methods, in turn, are obtained as a generalization of the explicit methods, by giving up the requirement that stages can be computed by means of forward substitution. Let us suppose that $\mathbf{k}_1, ..., \mathbf{k}_s \in \mathbb{R}^d$ satisfy the following nonlinear equations:

$$\mathbf{k}_1 = f(t_0 + c_1 h, \mathbf{y}_0 + h\sum_{\ell=1}^{s} a_{1\ell}\mathbf{k}_\ell) \tag{B.10}$$

$$\vdots \tag{B.11}$$

$$\mathbf{k}_s = f(t_0 + c_s h, \mathbf{y}_0 + h\sum_{\ell=1}^{s} a_{s\ell}\mathbf{k}_\ell) \tag{B.12}$$

for given coefficients $a_{i\ell}, c_i \in \mathbb{R}$. Then

$$\mathbf{y}_1 = \mathbf{y}_0 + h\sum_{i=1}^{s} b_i \mathbf{k}_i \tag{B.13}$$

is one step of the s-stage implicit Runge-Kutta method. The difference with an explicit method is in the definition of k_i for a generic i: in an explicit method, the sum over j only goes up to $i-1$.

The integration process comes with a number of issues which need to be handled carefully. One of these is the problem of *interpolation*, which was not originally included in early Runge-Kutta solvers. The custom was to step directly from one output point to the next one. However, it is possible to obtain more precise solutions by stepping beyond the point and obtaining interpolated solutions. This technique can now be handled with two different methods: Hermite interpolation and continuously embedded methods.

A second issue, which also becomes critical in the case of stiff equations, is that of setting a suitable step size for integration. The goal which stimulated some research in this direction was the need to obtain dense output without limiting the integration step size. Early software imposed a limit of the magnitude of the step size, setting it up not to be larger than the smallest delay. This clearly posed a problem since small delays are all but infrequent in DDEs problems, and the restriction on the step size can have important consequences on the efficiency of a solver. The modern solution to this problem is again to resort to interpolation polynomials, applying them in a precise way when the step size exceeds a delay.

In the case of stiff equations, the difficulty in the integration process is given by the wide relative difference between the speed scales of the system components. As for the FHN model, the stiffness is determined by the multiplicative factor ε, which in turn determines the difference in the time scales.

This marked difference implies that the equations need an elastic handling of the step size, so to obtain the same precision for the equations in spite of their different variation rate. Hence, it is essential to find a numerical method that poses no restriction on the integration step size of stiff equations. Not many of the commonly used methods have this kind of flexibility. To name one, Euler's method does pose such kind of restriction.

A concept that becomes relevant in this context is the *region of absolute stability* of the integration method. In particular, an integration method is said to be *absolutely stable* if all the roots of its stability polynomial satisfy a specific boundary condition. The region of absolute stability is the set of all points in the complex plane that make the method absolutely stable.

Explicit Runge-Kutta methods are not suitable for the integration of stiff equations because their region of absolute stability is quite small, while it becomes considerably larger in the case of implicit methods. The main issue with implicit methods, on the other hand, is the computational cost. An implicit linear multistep method requires the simultaneous solution of a number of equations equal to the number of equations of the system; an implicit Runge-Kutta method with s integration stages (called s-stage) also requires to multiply the mentioned computational bargain by an s-factor. To be fair, some techniques have been developed to improve the low efficiency of these methods [26].

To accomplish the differential equations system integration of the FHN model, we used the implicit Runge-Kutta method RADAR5, developed by Ernst Hairer and Nicola Guglielmi, partially modified by PhD student Giulio Colombini. The RADAR5 code is

written in ANSI Fortran-90 and is made of a number of routines, which constitute the kernel of the program.

The FHN model is an example of a problem with diagonal M, i.e., $M = \left(\begin{smallmatrix} \varepsilon & 0 \\ 0 & 1 \end{smallmatrix}\right)$. This feature characterizes it as a singularly perturbed problem, that is, an important class of stiff problems containing a small parameter that cannot be approximated to zero. In other words, the solution cannot be approximated by an asymptotic expansion.

The integration method RADAR5 is used for initial value problems of the following kind

$$M\mathbf{y}'(t) = \mathbf{f}(t, \mathbf{y}(t), \quad \mathbf{y}(\alpha_1(t, \mathbf{y}(t))), ..., \mathbf{y}(\alpha_m(t, \mathbf{y}(t)))), \tag{B.14}$$

$$\mathbf{y}(t_0) = \mathbf{y}_0, \quad \mathbf{y}(t) = \mathbf{g}(t) \text{ for } t < t_0, \tag{B.15}$$

where M is a constant dd matrix, that can be identified as the "mass matrix" of the problem, and $\alpha_i(t, \mathbf{y}(t)) \leq t$ for all $t \geq t_0$ and for all i. Matrices akin to M might be found in the discretization of partial differential equations with time delay. The M matrix is also allowed to be singular, that is, the case of ε being equal to zero. From a dynamical point of view, this causes a sharp discontinuity in the phase space. Numerically, even if integration is allowed in the singular case, the results do sometimes vary from the predicted behavior, making the simulations difficult to interpret.

The RADAR5 code is built on implicit Runge-Kutta methods, and specifically on collocation methods based on *radau nodes*, which are particularly suited to solve stiff problems. The main concept of collocation methods is to choose a finite-dimensional space of candidate solutions (usually polynomials up to a certain degree) and a number of points in the domain, called collocation points, and to select that solution which satisfies the given equation at the collocation points.

A subclass of the implicit methods, Radau IIA methods, was specifically developed for the numerical treatment of stiff and differential-algebraic problems, as they are known for their excellent stability properties when applied to stiff differential equations. Radau IIA methods are built as one-step methods of collocation type.

Some of the delicate issues handled by the code are the presence of small delays, as well as the existence of large elements in the derivative of the right-hand side of the system, with respect to the retarded argument. In particular, the delay theme becomes relevant when the delay is smaller than the step size. In that case, the theory for ODEs (which could be used in the opposite case) can no longer be applied. A general purpose code for stiff delay equations should be able to allow for step sizes larger than the delay, since the issue of efficiency of the code is linked to the possibility to use large step sizes.

An efficient solution of the nonlinear equations is in fact the most difficult target to reach in the implementation of implicit methods. For stiff problems (or when M is singular), this system cannot be solved by fixed point iteration, and one is obliged to use some kind of simplified version of Newton iterations.

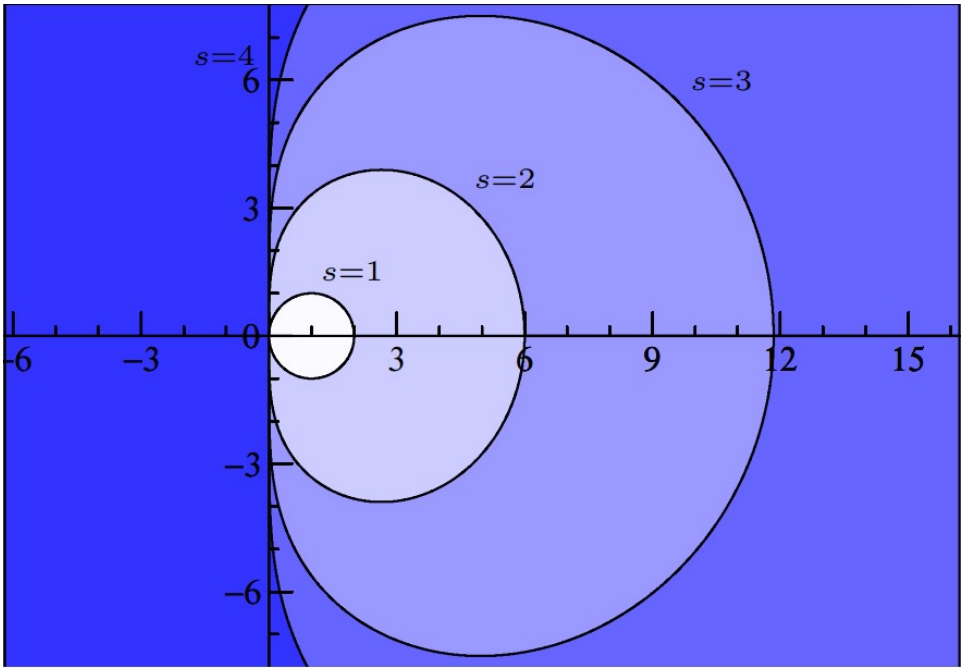

Figure B.1: Stability regions of Radau IIA methods. Here s indicates the degree of the polynomial $u(t)$ that satisfies $u(t_n) = y_n$. For $s = 1$ the method reduces to the implicit Euler discretization. Original by E. Hairer and G. Wanner [27]

In the RADAR5 code there is a focus on the individuation and handling of discontinuity points, i.e. the points where some right-hand derivative of the solution at t_0 is different from the corresponding left-hand derivative. As we have already seen, this kind of discontinuity might propagate along the integration interval, so its evolution needs to be handled with care. This kind of discontinuity points are found as *breaking points* in the code.

Bibliography

[1] Julius Bernstein. *Untersuchungen zur Thermodynamik der bioelektrischen Ströme: Erster Theil*. Nov. 1902.

[2] L. Lapicque. *Recherches quantitatives sur l'excitationelectrique des nerfs traitee comme une polarisation*. 1907.

[3] Robert G. Frank. "Instruments, Nerve Action, and the All-or-None Principle". In: *Osiris* 9.1 (1994). PMID: 11613429, pp. 208–235.

[4] Kenneth S. Cole and Howard J. Curtis. "Electrical Impedance of Nerve During Activity". In: *Journal of General Physiology* 22.5 (May 1939), pp. 649–670.

[5] Frederic B. Fitch. "Warren S. McCulloch and Walter Pitts. A logical calculus of the ideas immanent in nervous activity. Bulletin of mathematical biophysics, vol. 5 (1943), pp. 115–133." In: *Journal of Symbolic Logic* 9.2 (1944), pp. 49–50.

[6] Yang Kuang. "Delay Differential Equation with Application in Population Dynamics". In: (Jan. 1993).

[7] L. Berezansky, E. Braverman, and L. Idels. "Nicholson's blowflies differential equations revisited: Main results and open problems". In: *Applied Mathematical Modelling* 34.6 (2010), pp. 1405–1417. ISSN: 0307-904X.

[8] Thomas Erneux. *Applied Delay Differential Equations*. Vol. 3. Jan. 2009. ISBN: 978-0-387-74371-4.

[9] Sue Ann Campbell. "Time Delays in Neural Systems". In: *Handbook of Brain Connectivity*. Ed. by Viktor K. Jirsa and AR McIntosh. Berlin, Heidelberg: Springer Berlin Heidelberg, 2007, pp. 65–90. ISBN: 978-3-540-71512-2.

[10] Giulio Colombini. *Synchronisation Phenomena in Complex Neuronal Networks*. 2021.

[11] Richard FitzHugh. "Impulses and Physiological States in Theoretical Models of Nerve Membrane". In: *Biophysical Journal* 1.6 (1961), pp. 445–466. ISSN: 0006-3495.

[12] Richard Bertram. *Delay-Differential Equations*.

[13] Eugene M. Izhikevich. *Dynamical Systems in Neuroscience: The Geometry of Excitability and Bursting*. The MIT Press, July 2006. ISBN: 9780262276078.

[14] Original by en:User:Chris 73, updated by en:User:Diberri, converted to SVG by tiZom.

[15] Marios Tsatsos. "The Van der Pol Equation". In: (Apr. 2008).

[16] T. Kanamaru. "Van der Pol oscillator". In: *Scholarpedia* 2.1 (2007). revision #138698, p. 2202.

[17] S.H. Strogatz. *Nonlinear Dynamics and Chaos: With Applications to Physics, Biology, Chemistry, and Engineering*. 2nd ed. CRC Press, 2015.

[18] John Milnor. "On the concept of attractor". In: *Communications in Mathematical Physics* 99.2 (1985), pp. 177–195.

[19] Y. A. Kuznetsov. "Andronov-Hopf bifurcation". In: *Scholarpedia* 1.10 (2006). revision #90964, p. 1858.

[20] Andronov A. A. et al. *Theory of Bifurcations of Dynamical Systems on a Plane*. Translation. 1971, p. 496.

[21] Richard FitzHugh. "Mathematical models of threshold phenomena in the nerve membrane". In: *Bulletin of Mathematical Biology* 17 (1955), pp. 257–278.

[22] Richard E. Plant. "A Fitzhugh Differential-Difference Equation Modeling Recurrent Neural Feedback". In: *SIAM Journal on Applied Mathematics* 40.1 (1981), pp. 150–162. ISSN: 00361399.

[23] Giulio Colombini. *Private communication*. Sept. 2022.

[24] Cleve Moler. *Stiff Differential Equations*. MathWorks, Technical Articles and Newsletters. 2003.

[25] S. Thompson. "Delay-differential equations". In: *Scholarpedia* 2.3 (2007). revision #150987, p. 2367.

[26] Endre Süli and David F. Mayers. *An Introduction to Numerical Analysis*. Cambridge University Press, 2003.

[27] Ernst Hairer and Gerhard Wanner. "Radau Methods". In: Jan. 2015, pp. 1213–1216.